

THE UNIVERSITY OF MANITOBA

FACTORS INFLUENCING THE PROPERTIES OF
DUCTILE IRON CASTINGS

By

Khalid Iqbal

A Thesis
Submitted to the Faculty of Graduate Studies
In Partial Fulfillment of the Requirements for the Degree of
Master of Science

Winnipeg, Manitoba
1974

FACTORS INFLUENCING THE PROPERTIES OF
DUCTILE IRON CASTINGS

by

KHALID IQBAL

A dissertation submitted to the Faculty of Graduate Studies of
the University of Manitoba in partial fulfillment of the requirements
of the degree of

MASTER OF SCIENCE

© 1974

Permission has been granted to the LIBRARY OF THE UNIVERSITY OF MANITOBA to lend or sell copies of this dissertation, to the NATIONAL LIBRARY OF CANADA to microfilm this dissertation and to lend or sell copies of the film, and UNIVERSITY MICROFILMS to publish an abstract of this dissertation.

The author reserves other publication rights, and neither the dissertation nor extensive extracts from it may be printed or otherwise reproduced without the author's written permission.



ABSTRACT

The composition of a metal or alloy and the rate at which it solidifies (the solidification rate) have an important effect on its microstructure and mechanical properties. A study was made on the solidification of four castings made from commercial ductile iron to provide fundamental information which will enable the foundryman to predict the course of solidification and hence allow adjustment of variables to obtain the best mechanical properties.

The graphite morphology in commercial ductile iron was also studied. The effect of different variables such as cooling rate, metal charge and chemical composition were observed on the graphite and matrix structure of the metal.

It was found that the solidification rate had a marked effect on the size and concentration of the graphite nodules. The metal charge and chemical composition influenced the shape of graphite and matrix structure. The most significant effect on mechanical properties resulted from poorly shaped nodules caused by compositional deficiencies in the cast iron.

ACKNOWLEDGMENTS

I wish to express my sincere thanks to Dr. J. R. Cahoon for his patient guidance, supervision and constant encouragement during the course of this project. I am also indebted to the many staff members and students of the department for their helpful discussions and criticisms. I also wish to thank Mr. C. McBain, Mr. A. Hughes, Mr. Tom Liddell and Mr. Garry Nicholson for their advice and help. My thanks also goes to Mrs. R. Hanley for typing the thesis.

The financial assistance and practical help provided by Ancast Industries Limited (formerly Anthes Western Limited) is gratefully acknowledged.

TABLE OF CONTENTS

	<u>Page</u>
Figures and Illustrations	i
Index of Tables	iv
1. INTRODUCTION	1
2. THEORETICAL	2
2.1 General	2
2.2 Specifications for Ductile Iron Castings	2
2.3 Chemical Composition of Ductile Iron	5
2.3.1 Effect of Carbon and Silicon	5
2.3.2 Effect of Sulphur	6
2.3.3 Effect of Manganese	7
2.3.4 Effect of Magnesium	7
2.3.5 Effect of Phosphorus	8
2.3.6 Effect of Minor Elements	8
2.4 The Solidification of Nodular Iron	10
2.5 Melting Ductile Iron Base	12
2.5.1 Desulphurization	12
2.5.2 Carburization	13
2.5.3 Melt Temperatures	13
2.6 Charge Material for Ductile Iron	13
2.6.1 Control of Chemical Composition	14
2.7 The Mechanical Properties	14
2.7.1 Hardness	16
2.7.2 Tensile Properties	16

2.7.3	Properties Dependence on Microstructure	17
2.7.4	Effect of Chemical Analysis	17
3.	EXPERIMENTAL	19
3.1	Preparation of Melt	19
3.2	The Temperature Measurement	20
3.3	The Tensile Test	22
3.4	Chemical Analysis	26
3.5	Metallography	26
4.	RESULTS	28
4.1	Solidification Time and Cooling Rate	28
4.2	Chemical Analysis	35
4.3	Metallographic Observations	44
4.4	The Tensile Properties	54
5.	DISCUSSION OF RESULTS	59
5.1	The Effect of Charge Material	59
5.2	Solidification Time and the Effect of Section Size	61
5.3	The Chemical Composition	62
5.4	Metallography	64
5.5	The Mechanical Properties	65
6.	CONCLUSIONS	69
7.	BIBLIOGRAPHY	71

FIGURES AND ILLUSTRATIONS

<u>Fig. No.</u>	<u>Figure</u>	<u>Page No.</u>
1.	Approximate range in C-Si contents of Ferrous Alloys	3
2.	Relationship between elongation and yield strength of ductile iron	3
3.	Dependence of Carbon-Equivalent on Liquidus and Eutectic Arrest	15
4.	Thermocouples and Temperature Recording Arrangement for Wedge Shaped Castings During the Experiment	21
5(a).	Bottom Clevis	23
5(b).	Four Bottom Clevises casted together	23
6(a).	Picture Showing third wedge shaped ingot as cast	24
6(b).	Section arrangement in the first three wedge shaped castings	25
7(a).	Temperature distributions in ingot I	29
7(b).	Temperature distributions in ingots II & III	30
8(a).	Solidification time along the length of ingot I	31
8(b).	Solidification time along the length of ingots II & III.	32
9.	Time to reach 1000 ^o C, 900 ^o C and 700 ^o C temperature versus minimum section thickness for Ductile iron casting No. IV	34
10.	Carbon distribution along ingots No. I, II & III	38
11.	Silicon distribution along ingots No. I, II & III	39

12.	Sulphur Distribution Along Ingots No. I, II & III	40
13.	Manganese Distribution Along Ingots No. I, II & III	41
14.	Magnesium Distribution Along Ingots No. I, II & III	42
15.	Compositional Variations with Cooling Rate in Casting No. IV	43
16(b).	Microstructure of Normalized Ductile Iron Casting No. 1, Section B	45
16(c).	Microstructure of Normalized Ductile Iron Casting No. 1, Section C	45
16(d).	Microstructure of Normalized Ductile Iron Casting No. 1, Section D	46
16(e).	Microstructure of Normalized Ductile Iron Casting No. 1, Section E	46
16(f).	Microstructure of Normalized Ductile Iron Casting No. 1, Section F	47
17(b).	Microstructure of As-cast Ductile Iron Casting No. 2, Section B	47
17(c).	Microstructure of As-cast Ductile Iron Casting No. 2, Section C	48
17(d).	Microstructure of As-cast Ductile Iron Casting No. 2, Section D	48
17(e).	Microstructure of As-cast Ductile Iron Casting No. 2, Section E	49
17(f).	Microstructure of As-cast Ductile Iron Casting No. 2, Section F	49

18(b).	Microstructure of As-cast Ductile Iron Casting No. 3, Section B	50
18(c).	Microstructure of As-cast Ductile Iron Casting No. 3, Section C	50
18(d).	Microstructure of As-cast Ductile Iron Casting No. 3, Section D	51
18(e).	Microstructure of As-cast Ductile Iron Casting No. 3, Section E	51
18(f).	Microstructure of As-cast Ductile Iron Casting No. 3, Section F	52
19(a).	Microstructure of As-cast Ductile Iron Casting No. 4, Section A	52
19(c).	Microstructure of As-cast Ductile Iron Casting No. 4, Section C	53
19(e).	Microstructure of As-cast Ductile Iron Casting No. 4, Section E	53
20.	Yield Strength v/s Solidification Time for Ingots I, II & III	55
21.	Tensile Strength v/s Solidification Time for Ingots I, II & III	56
22.	Percent Elongation v/s Solidification Time for Ingots I, II & III	57
23.	Mechanical Properties of Casting No. IV, Bottom Clevis	58

INDEX OF TABLES

<u>No.</u>	<u>Title</u>	<u>Page No.</u>
1.	Commonly Specified Grades of Ductile Iron	4
2.	Structural Effects of Some Elements in Ductile Iron	8
3.	Charge Used for the Production of Ductile Iron	19
4.	Solidification Times for Ingots I, II & III	28
5.	Cooling Rates for Ingot No. IV	33
6.	Chemical Analysis of Ingot No. I	36
7.	Chemical Analysis of Ingot No. II	36
8.	Chemical Analysis of Ingot No. III	37
9.	Chemical Analysis of Ingot No. IV	37

1. INTRODUCTION

Local foundries have considerable difficulty in producing ductile iron casting with consistent properties; as a result, many castings with obvious deficiencies must be remelted in the foundry. But many deficient castings are sent to users which subsequently fail in service. Many ductile iron castings, for example, produced in Winnipeg for local farm machinery producers have failed in service, and subsequent failure analysis has shown that the castings were of poor quality.¹

The production of good quality ductile iron requires much tighter quality control as compared to other types of iron and steel. Facilities for rapid and complete chemical analysis of the melt are necessary to be absolutely sure of the resulting alloy. Such facilities are expensive and beyond the capability of small foundries.

An investigation was, therefore, initiated to determine the factors most important in controlling the properties of ductile iron, with the purpose of establishing the minimum quality control necessary to produce castings of consistent and adequate properties. This work was done in cooperation with a local foundry, Anthes Western Ltd., now Ancast Industries Ltd.

Several castings of experimental shape were made to establish the important factors controlling the mechanical properties of ductile iron, and these results were used in predicting the properties in some commercial castings.

2. THEORETICAL

2.1 General

Ductile iron is the latest addition to the family of ferrous alloys, the broad limits of chemical composition of which are shown in figure 1. As early as 1936 it was reported that gray cast iron can exhibit nodular-shaped graphite instead of the common flake-like graphite by using a suitable heat treatment. In 1947 it was shown by Morrogh^{2,3} that the shape of graphite in cast iron can be modified from flake morphology to a nodular one without any heat treatment. This morphological change is usually obtained by the addition of oxide forming elements like Mg, Ca, Ce, Na, K, and Be,⁴ generally called as nodulizers.

2.2 Specifications for Ductile Iron Castings

Ductile irons, like other ductile materials, are specified by their mechanical properties. The general specification for ductile iron castings ASTM A 536 - 65 T June, 1965⁵ and A 536 - 70 T⁶ has requirements shown in table I.

The mechanical properties of the metal are dependent on the matrix structure (figure 2) and on the shape and size of the graphite nodule and hence are sometimes classified according to microstructure.⁵

It is of interest to mention here that in the Soviet Union,⁷ along with the classifications mentioned above, Soviet State Standard classifies nodular iron according to the microstructural area percentage occupied by graphite particles or according to the graphite particle size.

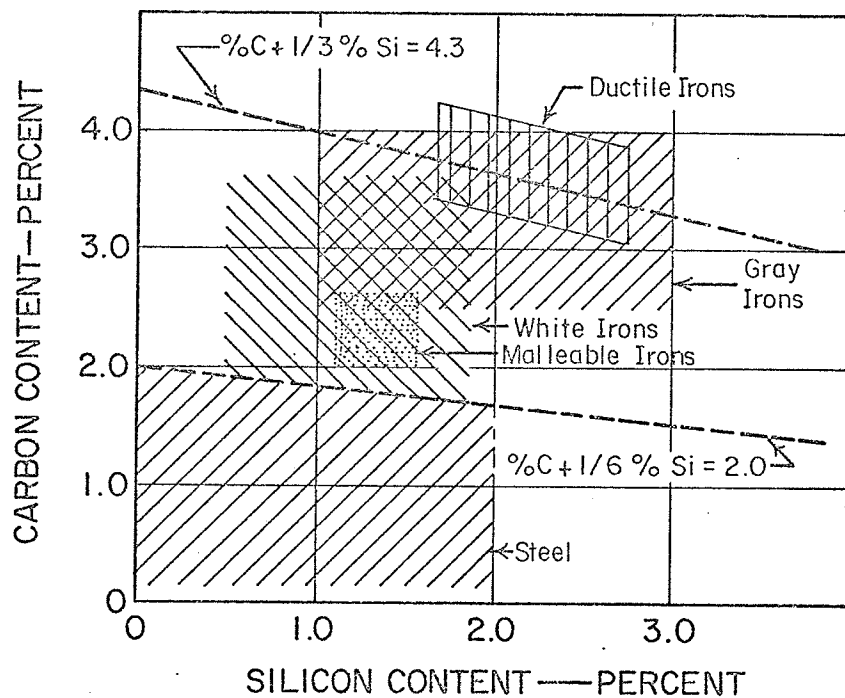


FIG. 1 THE APPROXIMATE RANGE IN CARBON & SILICON CONTENTS OF FERROUS ALLOYS

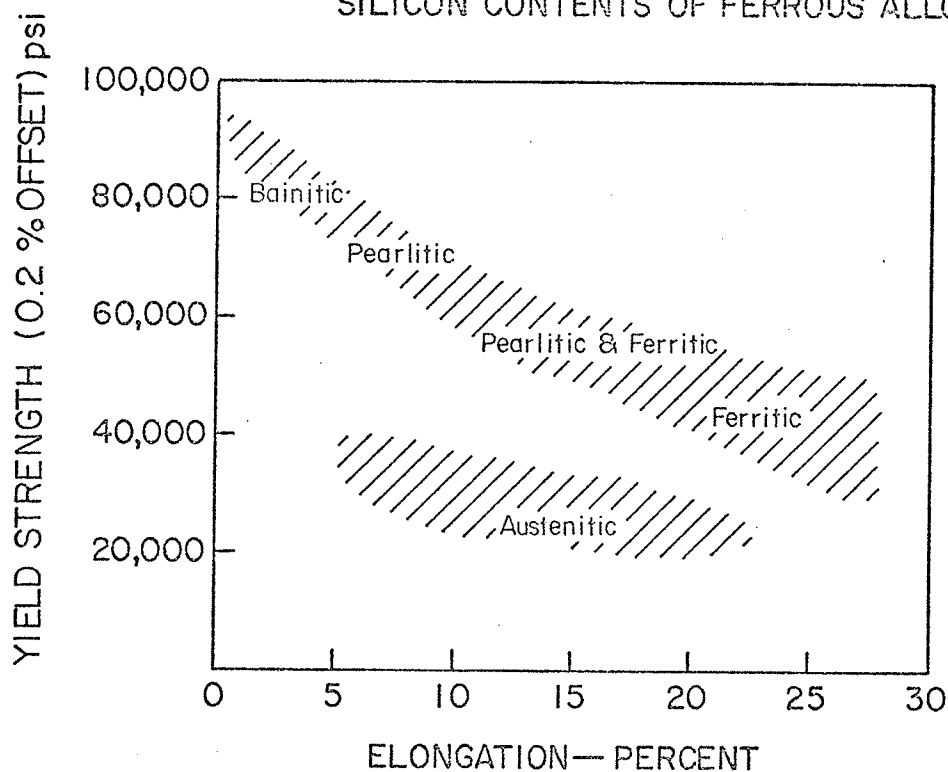


FIG. 2 RELATIONSHIP BETWEEN ELONGATION & YIELD STRENGTH OF D. I.

TABLE I

COMMONLY SPECIFIED GRADES OF DUCTILE IRON

Grade	Heat Treatment*	Tensile Str. minimum psi	Yield Str. minimum psi	Minimum % Elongation in 2" G.L.	Brinell Hardness	Matrix micro-structure
60-40-18	1	60,000	40,000	18	149-187	Ferrite
65-45-12	2	65,000	45,000	12	170-207	Ferrite + pearlite
80-55-06	3	80,000	55,000	6	187-255	Pearlite + ferrite
100-70-03	4	100,000	70,000	3	217-269	Pearlite
120-90-02	5	120,000	90,000	2	240-300	Tempered Martensite

* Heat Treatment:

1. May be annealed after casting
2. Generally obtained as cast
3. An as cast grade with higher Mn content
4. Usually obtained by a normalizing heat treatment
5. Oil quenched and tempered to desired hardness

2.3 Chemical Composition of Ductile Iron

Chemical composition is one of the variables that exerts a major influence on the structure and properties of ductile iron. Keeping other variables, such as cooling rate, melting temperature, inoculation, etc., constant chemical composition influences ductile iron in two ways:

- (a) Mode of solidification
- (b) Matrix structure.

Depending on the mode of solidification, ductile iron may freeze with spheroidal graphite or flake or other deteriorated graphite shapes. Also it may or may not be free of carbides.

Depending on the matrix structure, ductile iron may exhibit mechanical, chemical and physical properties over a wide range as is obvious from figure 2 and table I.

The effects of different elements present in ductile iron are discussed in detail below.

2.3.1 Effect of Carbon and Silicon

These are the only two elements which strongly promote carbide free, as-cast structure. Increasing the carbon and/or silicon content of iron results in a lowering of the melting point. The lowest melting point alloys are those having the eutectic composition or when the carbon equivalent which is given by

$$\text{C.E.} = \%C + \frac{1}{3} \%Si = 4.3 \quad (1)$$

Other values representing carbon equivalent of cast iron have also been suggested. When an appreciable amount of phosphorus is present it is also included in the expression as is shown below

$$\text{C.E.} = \%C + \frac{1}{3}(\%Si + \%P) \quad (2)$$

Some authors⁶ prefer to express it in terms of the degrees of saturation of the iron which is given by

$$S_c = \frac{\%C}{4.3 - \frac{1}{3}(\%Si - \%P)} \quad (3)$$

S_c is equal to 1.0 for the eutectic composition (C.E. = 4.3). The alloy is hypo-eutectic for S_c less than unity and hyper eutectic for S_c greater than 1.0.

The upper limits of carbon and silicon are set by the solubility of carbon in liquid iron (floatation) and by the increasing brittleness due to increasing silicon content.

2.3.2 Effect of Sulphur

Free sulphur has been shown to be a deleterious element in the nodule growth and to hinder nodule formation. The sulphur content must be very low (less than 0.03%) to avoid excessive reaction with magnesium which is not only an excellent desulphurizer but is also necessary to form spheroidal graphite. Magnesium reacts with sulphur forming MgS (magnesium sulphide) until the sulphur content is below 0.01% and is at equilibrium with magnesium in iron. Irons with a low sulphur content graphitize almost

completely.^{8,9} Commercial gray or ductile iron has a pearlitic structure with 0.06 to 0.25%S. Sulphur does not have any detrimental effect on cast iron as it has on the hot working of steel. In absence of manganese, sulphur combines with iron to form iron sulphide FeS in the grain boundaries during solidification.

2.3.3 Effect of Manganese

Though itself a mild carbide and pearlite former, when present in sufficient amounts with sulphur it forms manganese sulphide particles in the microstructure which acts as nucleation sites for graphite nodules.⁸ It may be possible to grain refine ductile cast iron by controlling the MnS formation or addition. Ductile irons containing many small nodules or a few large ones could be produced without the necessity of changing other factors such as the cooling rate. The balance of sulphur and manganese contents that will neutralize each other and promote a maximum amount of free ferrite which is found to be,⁶

$$17 \times \%S + 0.15 = \%Mn. \quad (4)$$

2.3.4 Effect of Magnesium

Not all the magnesium present in the solid iron acts as a graphite spheroidizer. Magnesium combined with sulphur is rather inactive. Magnesium itself is a very potent carbide promoter when present in quantities more than that necessary for producing spheroidal graphite the carbide forming tendency is greatly increased.

In ductile iron magnesium is used as a graphite spheroidizer only and never as an alloying element.

2.3.5 Effect of Phosphorus

Phosphorus decreases ductility, toughness and weldability. In solution it tends to stabilize pearlite. If present in sufficient quantity in annealed or ferritic grades of ductile iron, it increases the impact transition temperature, the temperature below which an impact fracture tends to be brittle rather than ductile. For this reason the phosphorus content of the high ductility grades is generally limited to a maximum of 0.08 percent.

2.3.6 Effect of Minor Elements

Small amounts of a few of minor elements have an important influence on the properties and microstructure of the metal.¹⁰ Structural effects of some elements in cast iron are listed in table II.

TABLE II

STRUCTURAL EFFECTS OF SOME ELEMENTS IN DUCTILE CAST IRON

Element	Maximum percent permissible	Effect during Solidification	Effect during Eutectoid Reaction
Aluminium	0.10 ^a	Strong graphitizer	Promotes ferrite and graphite formation
Antimony	0.002	Little effect in amounts used	Strong pearlite retainer
Arsenic	0.02 ^b	-	-
Bismuth	0.002	Carbide promoter but not carbide former	Very mild pearlite stabilizer
Cadmium	0.01	-	-
Chromium	-	Strong carbide former. Forms very stable complex carbides	Strong pearlite former

Table II (Cont'd)

Element	Maximum percent permissible	Effect during Solidification	Effect during Eutectoid Reaction
Copper	-	Mild graphitizer	Promotes pearlite formation
Lead	0.002	-	-
Manganese	-	Mild carbide former	Pearlite former
Molybdenum	-	Carbide former	Strong pearlite former
Nickel	-	Graphitizer	Mild pearlite promoter
Selenium	0.03	-	-
Silicon	-	Strong graphitizer	Promotes ferrite and graphite formation
Tellurium	0.02 ^c	Very strong carbide promoter but not stabilizer	Very mild pearlite stabilizer
Tin	-	Little effect with amounts used	Strong pearlite retainer
Titanium	0.10 ^d	Graphitizer	^e Promotes graphite formation
Vanadium	-	Strong carbide former	Strong pearlite former
Zinc	0.10	-	-
Zirconium	0.10	Strong carbide former	-

- a) Much less than the content indicated here may cause pinholes under certain conditions.
- b) A combination of 0.1% arsenic and 0.003% cerium has been found to be beneficial in improving graphite structural and high temperature mechanical properties.
- c) Less than the quantity indicated here is sometimes added purposely to eliminate pinholes.
- d) Titanium is harmful in even smaller quantities as it decreases the range of magnesium contents for which fully spheroidal graphite structure can be obtained.
- e) Titanium is normally a carbide former but in small amounts the TiC formed may act as nuclei for graphite formation.

2.4 The Solidification of Nodular Iron

The solidification of nodular cast iron is a nucleation and growth process. Although graphite commonly appears as flakes in commercial Fe-C-Si alloys it is not the normal growth morphology of graphite. It has been shown^{8,9} that graphite tends to grow as nodules if the melt is free of impurities. It is generally accepted that certain subversive elements particularly free sulphur, which are found in commercial iron hinder the formation of spherulite. The nodularizing elements are believed to neutralize the effect of these subversive elements.

The growth of the austenite-graphite eutectic has been studied by several investigators.^{8,11-20} The most obvious method used was to interrupt the normal solidification reaction by rapid quenching at various stages and examining the microstructure metallographically.

It is now generally agreed that the metastable eutectic is not involved, but that the nodular graphite forms directly during the solidification; though there are conflicting results concerning the growth of graphite spherulites.

Morrough¹¹ working on magnesium-containing hyper-eutectic cast iron concluded that the hyper-eutectic spherulites separate directly from the melt without the formation of any other solid, but the growth of eutectic graphite occurs inside an austenitic shell.

Jolley,¹⁶ and Looper and Heine¹⁷ also reported that growth proceeds by the diffusion of carbon to the nodule from the liquid phase through the austenite shell.

The other theory is that the graphite nodule is nucleated in the liquid phase and starts to grow in contact with it, but at some later stage becomes enveloped by an austenite shell and the subsequent growth occurs by diffusion of carbon through the shell. This theory is discussed by Wetterfall, Fredriksson and Hillert¹¹ in their recent publication. They even obtained a microstructure immediately after the start of the eutectic reaction with graphite nodules without austenite shell, floating in the melt.

The conflicting results about the austenitic shell may be due to the differences in effectiveness of the quench and it is quite possible that an austenite shell develops during the quench. The possibility of nucleation of graphite and its initial growth in the melt was also suspected by Morrogh¹⁵, though he was not sure of it.

Schöbel studied nodules, which had austenite shells before the quench by measuring quantitatively the nodule size and the thickness of the shell and was able to deduce that there was at least a fraction of nodules which must have grown to a measureable size before becoming enveloped by an austenite shell.

Initially the nodule growth rate is controlled by the diffusion of carbon in the liquid phase, while after the formation of the austenite shell the growth continues to a much larger size but at a considerably lower rate¹¹. It was pointed out by Hillert and Lange¹² that the growth rate should be 20 times greater when controlled by diffusion through liquid as

compared to austenite, provided that the temperature, diffusion distance and carbon activity difference are the same.

2.5 Melting ductile iron Base

Iron ready to undergo magnesium treatment can be melted in all types of furnaces devised for iron and steel. By far the largest quantities are melted in cupola and induction furnaces.

2.5.1 Desulphurization

Ductile iron base as tapped from an acid cupola contains 0.08 to 0.12% sulphur, which has to be desulphurized to a lower percentage. Desulphurization by magnesium treatment though still in use is not recommended because of its high cost and, also, not all of the magnesium sulphide MgS and oxides of magnesium go into the slag. Other desulphurizing agents often recommended are calcium carbide CaC_2 , soda Ash Na_2CO_3 and lime CaO . There is a slight carbon pickup when using CaC_2 and a slight loss with Na_2CO_3 and CaO as shown by the following chemical reactions:



Some mechanical stirring is required in all the methods of desulphurization causing a temperature loss from 50° to 150°F .

2.5.2 Carburization

Carburization is recommended as a temporary practice, for the recovery of carbon is unpredictable, being dependent on many variables including temperature, method, carbon source, etc. Electrode carbon or graphite with low sulphur content is most commonly used as carbon raisers. Should a simultaneous increase in silicon content be desired one may consider the use of silicon-carbide.

2.5.3 Melt Temperatures

The optimum melting temperature is determined by the desired pouring temperature and the operational heat losses. The charged carbon (graphite or in any other form) goes into solution moments after melt down. Unnecessary super heat and long holding times are not recommended because of high cost and possible carbide formation.

2.6 Charge Material for Ductile Iron

Undesirable subversive trace elements in ductile iron can be obtained from charge material. These subversive elements exert a detrimental influence by altering both the growth characteristics of graphite nodules and the structure of the matrix. In ductile iron, trace elements cause the spherulitic nodules to degenerate into quasi-flake forms. These modified graphite shapes may lead to a serious loss of strength and ductility. In addition, changes in the matrix of the alloy also influence the mechanical properties.

The availability of low manganese, good steel scrap of known quality is a major factor in the charge selection. Out of the three main charge components the pig iron, ductile iron return and steel scrap, a greater use of the latter makes the control of the chemical composition more difficult. The usual controlling factor is the manganese content of steel, which, if high, has to be diluted by an equivalent amount of pig iron (sorel metal). This dilution also helps in controlling other undesirable elements either carbide stabilizers like Cr, V, etc., or impurities like Pb, Ti, etc.

Ductile iron scrap originating in the foundry is a prime quality charge material because of its known composition. Use of gray iron scrap is not recommended.

2.6.1 Control of Chemical Composition

The control of chemical composition of known quality charge is usually limited to the determination of combined carbon and silicon composition, or to the carbon equivalent only. Complete analysis is required in the case of unknown quality charge.

The measurement of the carbon-equivalent is based upon the dependence of the liquidus - solidus interval of cast-iron on the carbon equivalent as shown in figure 3.

2.7 The Mechanical Properties

Ductile iron provides a unique set of properties, combining the excellent casting properties and machinability of gray iron, with excellent

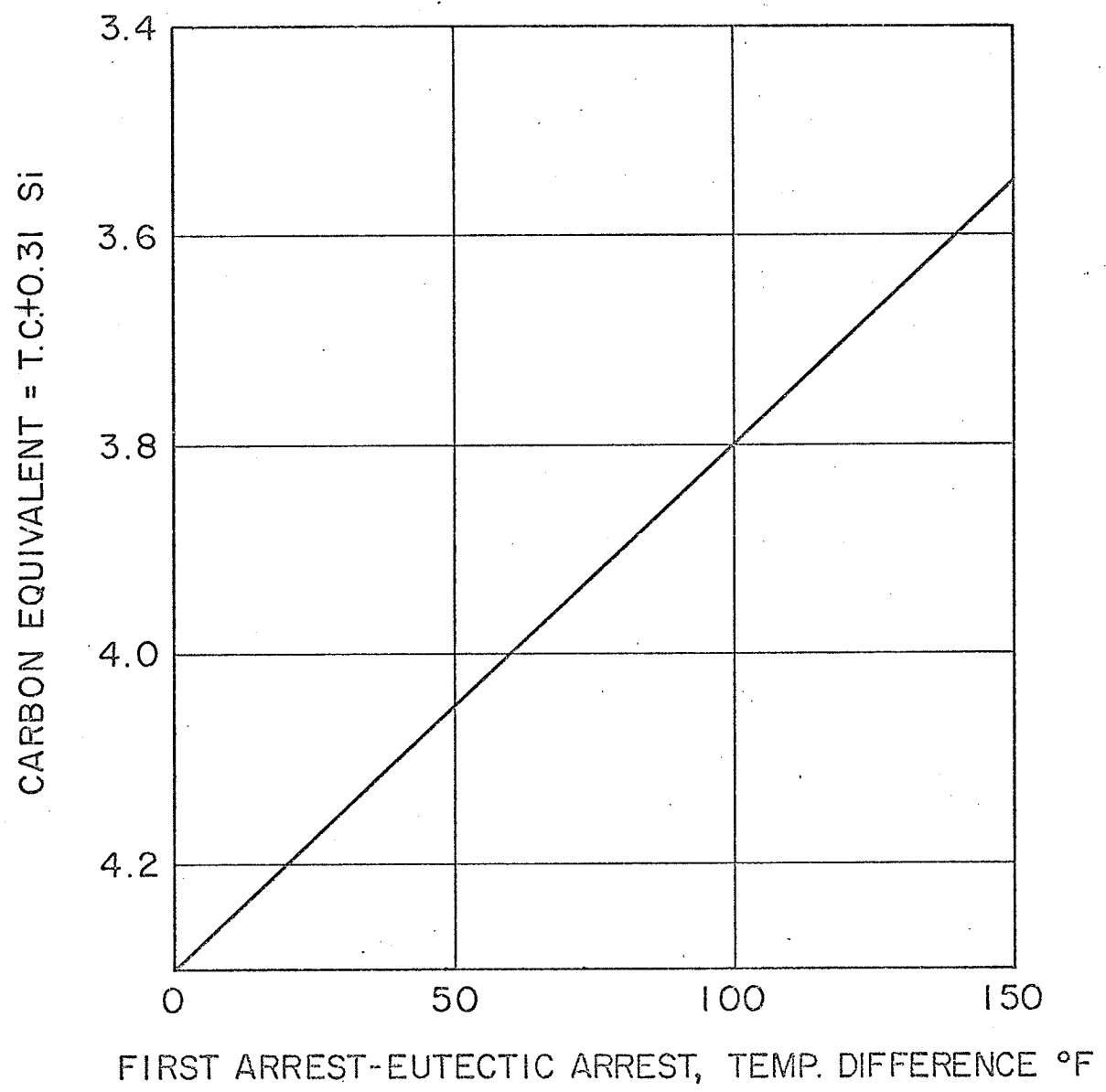


Fig.3 CARBON EQUIVALENT v/s LIQUIDUS SOLIDUS TEMPERATURE INTERVAL

mechanical properties including high strength high modulus of elasticity and ductility which are comparable to those of malleable iron and steel.

The mechanical properties of ductile iron are not specific to a batch or heat as is its chemical analysis. Properties are influenced by the microstructure, section thickness, and the manner in which the metal solidifies and cools.

The shape of graphite nodules affects the ductility of the metal. Hardness in ductile iron is a good indication of machinability. However, if the microstructure contains some free carbides, the machinability is reduced much more than indicated by the small increase in hardness.

As indicated above, the mechanical properties of ductile iron are directly influenced by the rate of solidification and subsequent cooling rate. Because of this, large and small castings from the same ladle of metal can have different mechanical properties. The casting designs were selected for our experiments keeping this property dependence in mind.

2.7.1 Hardness

The hardness of all graphite irons is essentially the hardness of the matrix reduced to a somewhat lower value due to the presence of the graphite.

2.7.2 Tensile Properties

The ultimate or tensile strength, yield strength and percent elongation or, in general, the tensile test results as they are called are the most important properties because they are used as the basis of most specifications for ductile irons as is obvious from table I.

2.7.3 Properties dependence on microstructure

Because of the nominal and consistent influence of the spheroidal graphite, the microstructure of the matrix establishes the properties of ductile iron as discussed below.

(a) Ferritic matrix irons, often annealed, with a very low combined carbon content are highly ductile. The hardness and strength are dependent upon hardening of ferrite by the elements dissolved in it of which silicon is the most important. Manganese and nickel are also common ferrite hardeners.

(b) Pearlitic matrix irons, in which lamellar carbide is the principal hardening agent.

(c) A uniform matrix of tempered martensite produced by heat treatment provides a somewhat higher strength to hardness relation.

(d) The alloyed acicular matrix irons have a similar relation, but generally have a lower ductility at a given strength.

2.7.4 Effect of Chemical Analysis

The chemical analysis of ductile iron has a direct effect on its tensile properties by influencing the type of matrix structure that is formed in the normal cooling of the casting or as the result of heat treatment.

In commercial practice an analysis of low in pearlite stabilizing elements like manganese are used for softer grades of ductile iron.

The higher strength grades with martensitic matrix calls for an analysis that will provide sufficient hardenability to respond satisfactorily to the cooling methods being used. Alloying elements may be necessary for heavy castings.

3. EXPERIMENTAL

3.1 Preparation of Melt

Since it was desired to work on commercial ductile iron, the metal charge was the same as commonly used in the foundry. Two different charges were used for the four castings made and are tabulated in Table III.

TABLE III

CHARGE USED FOR THE PRODUCTION OF DUCTILE IRON

Charge Components	Quantity per single Charge	
	Casting 1 & 2	Casting 3 & 4
Scrap Steel	500 lbs.	350 lbs.
Pig Iron (Sorel Metal)	100 "	200 "
Foundry Returns (Ductile Iron)	350 "	400 "
9 % Mg	12 "	15 "
50% FeSi	20 "	19 "
85% FeSi	4 "	5 "
Carbon (D-1 grade)	22 "	15 "

The melt was prepared in a 180 cycle per second induction furnace which had a lining of seunsk silicon (crushed silica quartz with boric acid as a binder). The alloy was given an open ladle spheroidizing treatment with magnesium. Nine (9) percent Magnesium alloy (approximate composition 9% Mg, 46% Si, 42% Fe) was placed on the bottom of the empty ladle and liquid iron was poured on top of it. To avoid the violence of the reaction, i.e., burning and boiling of magnesium, it was diluted by ferro-silicon alloy, called a non-violent carrier.

3.2 The Temperature Measurements

Since the value of the work depended upon the accuracy of the temperature measurements a careful study of the different techniques was made²¹ and the most suitable technique for the experiment was selected. Thermocouples were made from 1.5 mm diameter Chromel-Alumel wires welded together by oxy-acetylene flame and were enclosed in 7 mm. diameter twin bore silica tubing. One (1) cm. diameter hollow graphite tubings with one end closed were used to protect the thermocouples from molten metal.

The temperature readings were recorded in millivolts by means of a Rikadenki Kogyo electronic recorder (model B-104). The recorder was zeroed prior to recording corresponding to room temperature reference of 25°C as was observed at the time of pouring. The full scale deflection was of 100 mv corresponding to 2460°C. The chart speed was varied in fixed steps between 150 mm/min. to 50 mm/min.

A six way manual switch was used to connect the thermocouples to the recorder. The temperature readings in millivolts were taken at 3 to 10 second intervals depending on the chart speed.

Single piece green sand molds were prepared for the wedge-shaped castings, which were open from the top. One cm. diameter holes were drilled in the mold along the centre of the wedge section at 2" (5.08 cm.), 6" (15.24 cm.), 10" (25.40 cm.), 13" (33.02 cm.), 16" (40.64 cm.) and 18-1/4" (46.36 cm.) distances from the top as shown in figures 4 and 6. Thermocouples in graphite protector tubings were tightly fitted in the holes with their tips in the central axis of the ingot.

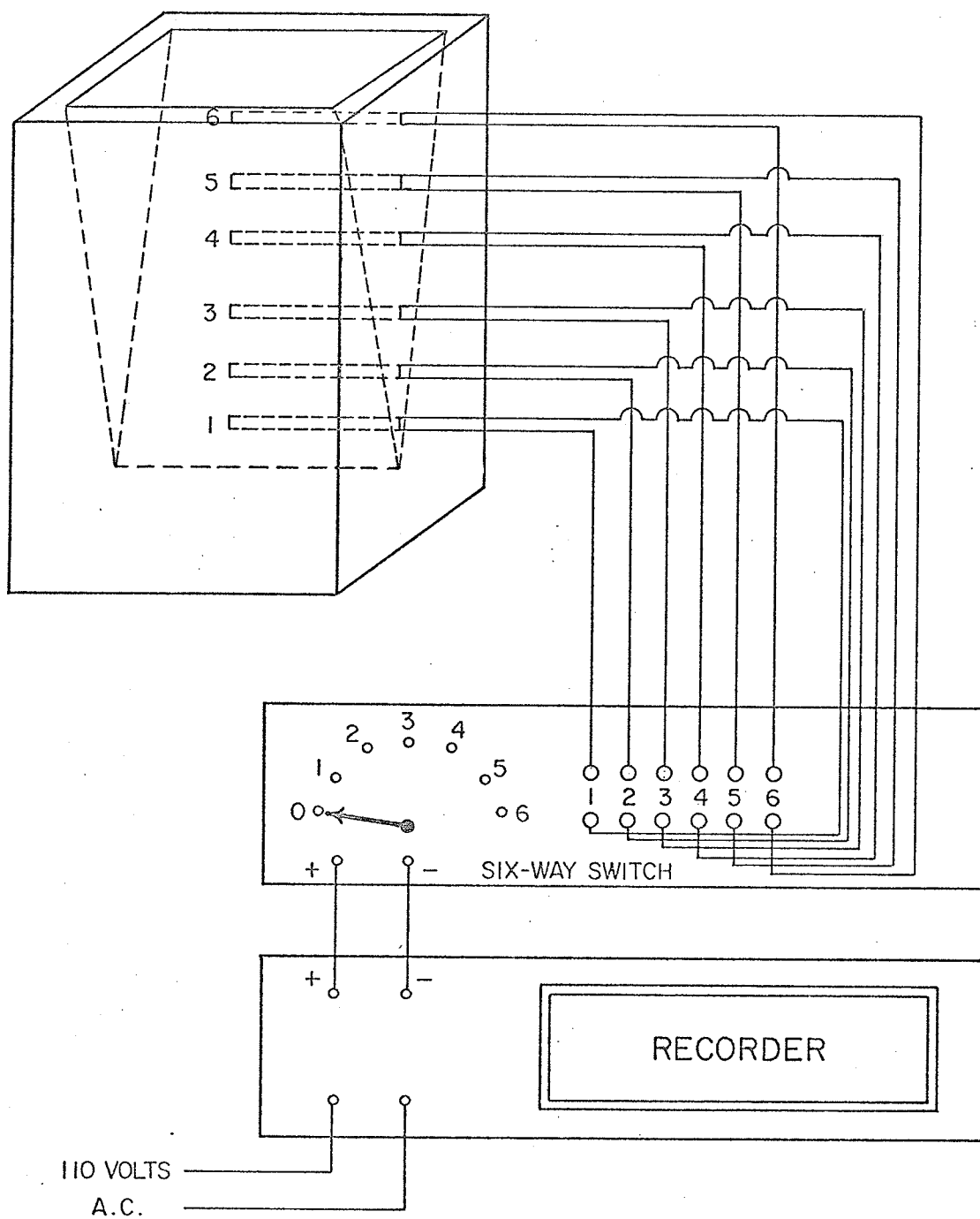


Fig. 4 THERMOCOUPLE ARRANGEMENT AND RECORDING EQUIPMENT FOR WEDGE SHAPED CASTINGS

Second and third ingots were cast under similar conditions using the same type of mold and mold material, the same pouring temperature and the same cooling conditions. It was, therefore, assumed that they would have the same cooling rate. The temperature readings were recorded only for the second ingot and similar values were assumed for the third one.

The first casting was kicked out of the mold after 66 minutes before the eutectoid transformation was complete, whereas the last two were left overnight within the mold to cool down to room temperature.

The fourth casting was a bottom clevis for an hydraulic machine, and was chosen because of its variety of section size in design. Two identical green sand molds were prepared, each in two pieces, cope and drag. Once again, 1 cm. diameter holes were drilled in one mold as shown in figure 5, to facilitate the placement of thermocouples. Because of space limitation no hole could be drilled in section c of the casting and cooling times for various temperatures were later obtained by the time vs. section size curve. A one inch minimum section keel block was also made from the same melt to compare its properties with the actual castings. Once again the castings were left overnight in the molds to cool down to room temperature.

3.3 Tensile Test

The wedge shaped ingots were divided into five sections B, C, D, E and F as shown in figure 6. Three different size sections were obtained from the bottom clevis A, C, and E as shown in figure 5. Each of the first three ingots yielded ten specimens, two from each of the five sections.

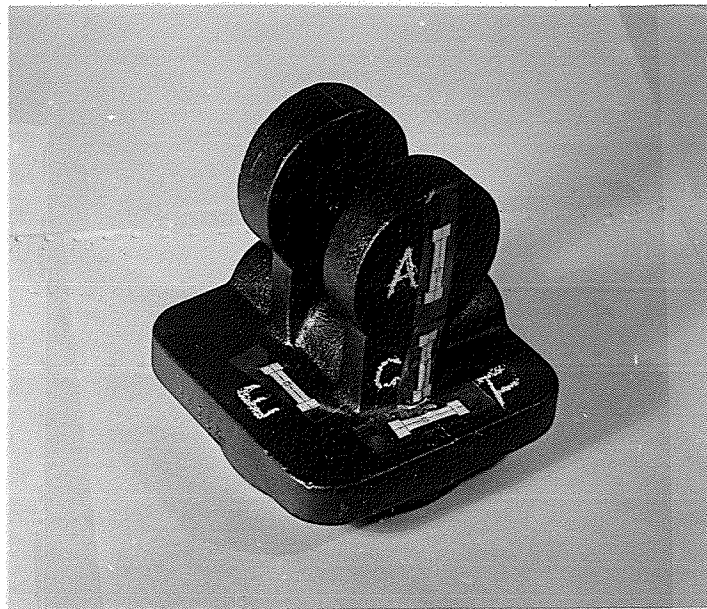


Fig. 5-a: Section arrangement in Bottom Clevis, ingot IV.

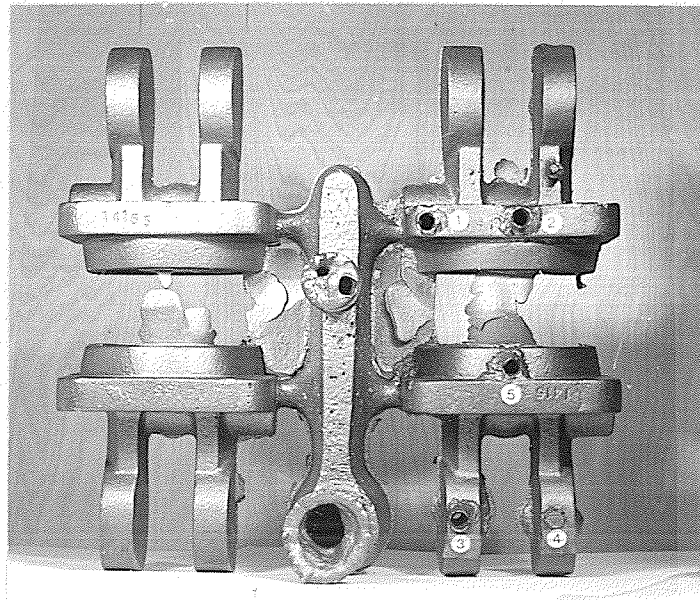


Fig. 5-b: Four Bottom Clevises, cast together. The numbers represent the arrangement of the thermocouples.

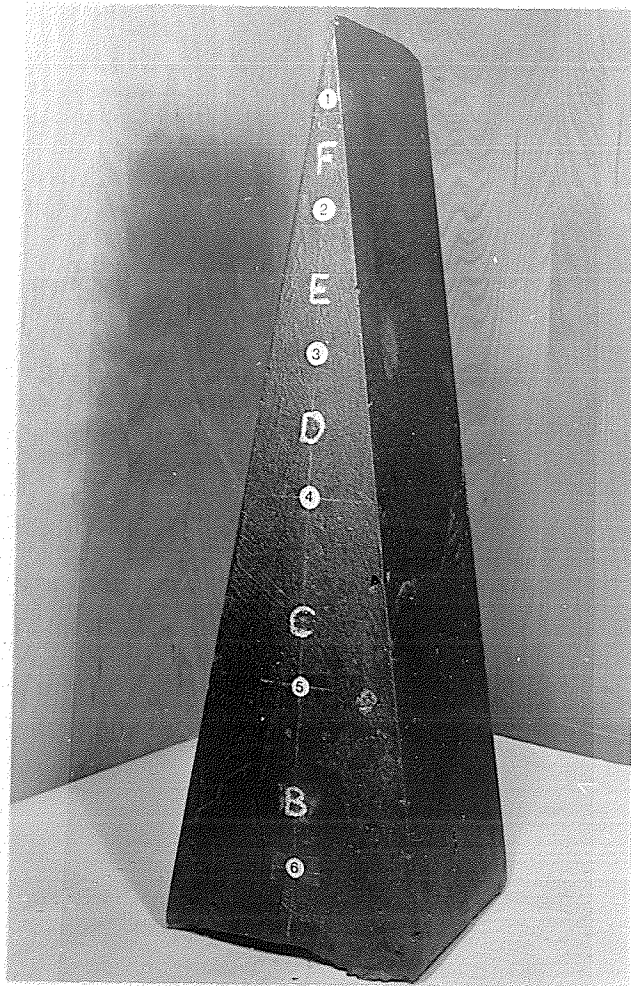


Fig. 6-a: Section arrangement in the first three wedge-shaped ingots.

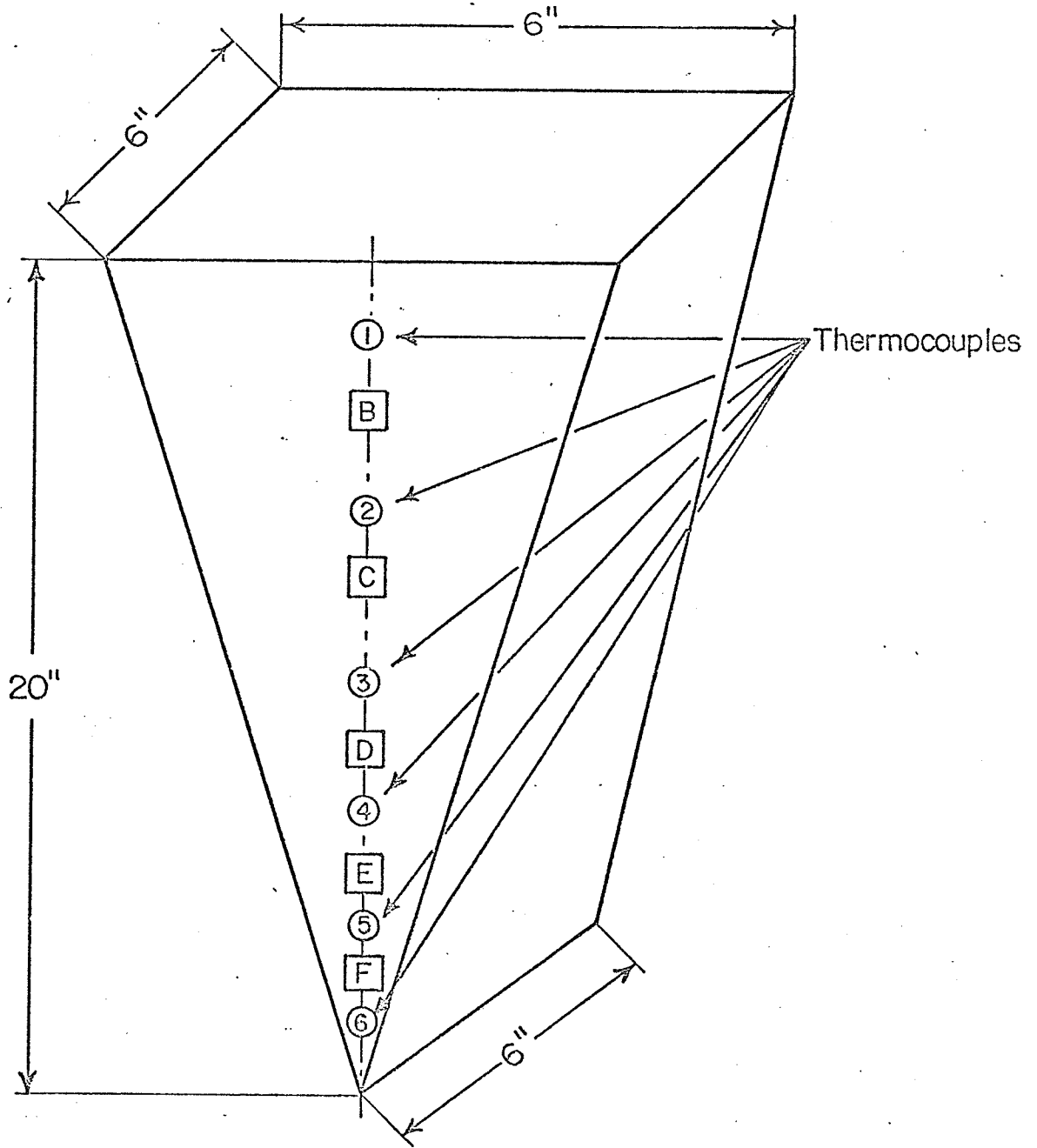


Fig. 6-B Section and thermocouples arrangement in the wedge shaped castings.

Six specimens were obtained from the fourth one, again two from each of the three sections.

Three-quarter inch square sections were cut by the help of a power saw and hand saw from the central part of different sections of the ingots where the structure was most uniform. Care was taken to keep the metal cool to retain the original as-cast structure. Different section arrangements are shown in figure 6.

Since the first ingot was removed from the mold before the eutectoid transformation was complete throughout, all tensile specimens were given a normalizing treatment (1 hr. at 900°C followed by air cooling) to ensure that all specimens had undergone similar heat treatment. All other ingots were tested in the as-cast condition.

Standard tensile specimens of 0.252" diameter and 1.25" gauge length were machined for each section and tested on Universal Instron Tensile Testing Machine floor model TTD. A GRM Load cell was used with full scale deflection of 200 kg.

3.4 Chemical Analysis

Drillings were obtained by 1/2" drill from the centre of each specimen section and were chemically analysed to obtain carbon, silicon, sulphur, manganese, and magnesium content.

3.5 Metallography

The fractured tensile specimens were cut by friction saw into about 1 cm. long pieces and mounted both horizontally and transversely in plastic molds. Once again special care was taken to keep the samples cool while cutting to retain the original microstructure.

Polishing was done in three stages. Initially four grades of silicon carbide waterproof paper was used in the following sequences: No. 220, 320, 400 and 600. Intermediate rough polishing was done using diamond abrasives in sequences of 6, 1 and 1/4 micron on synthetic suede cloth. Paraffin oil was used as a lubricant. The final polishing was done on linde B polishing wheel using 0.05 micron aluminum oxide AlO_2 suspended in water as abrasive. To avoid contamination the specimens were washed with tap water after every polishing stage.

Etching was done using 3% Nital (3 percent nitric acid in ethanol) for 5 to 10 seconds. The samples were then rapidly dried using hot air to avoid staining.

4. RESULTS

4.1 Solidification Time and Cooling Rate

The temperature distributions along the length of the ingot at different times, for the three wedge shaped castings are plotted in figure 7 (a and b). As expected from the shape of the ingot, the eutectic arrest and hence the solidification time was very small for section F and increased as the wedge section became larger from F to B. The solidification times along the ingot length are shown in figure 8 (a and b) and are also tabulated in Table IV.

TABLE IV
SOLIDIFICATION TIMES FOR INGOTS I, II & III

Section	Solidification Time for Ingot		
	I	II	III
B	1000 sec	2800 sec	2800 sec
C	1200 "	1000 "	1000 "
D	900 "	400 "	400 "
E	400 "	220 "	220 "
F	80 "	160 "	160 "

The solidification times for the first casting particularly for Section B were less than those for the second and third ones because the latter were covered on top by bricks immediately after pouring, thus minimizing heat losses, whereas the first casting was left open.

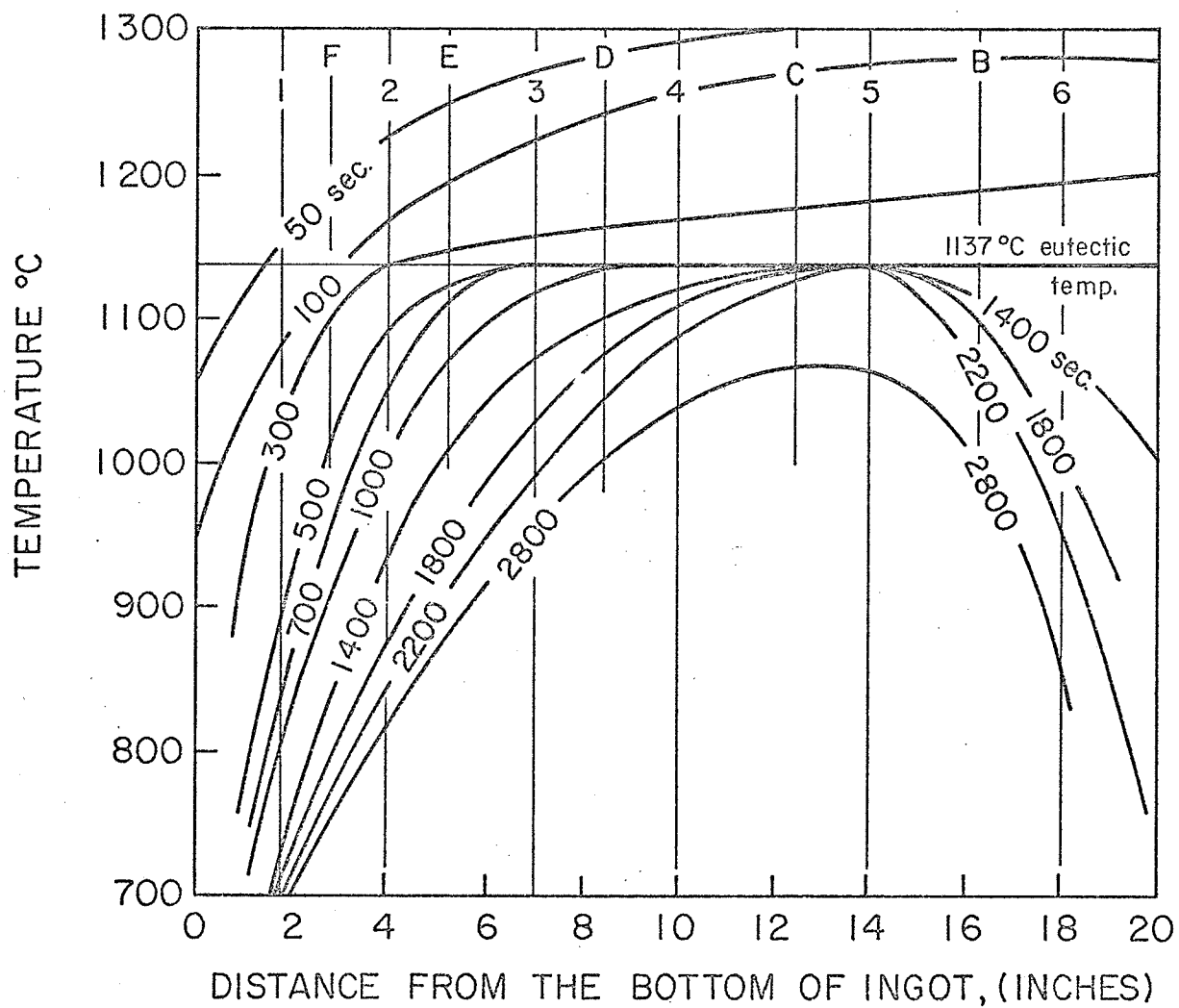


Fig. 7-a TEMPERATURE DISTRIBUTIONS IN INGOT NO. 1

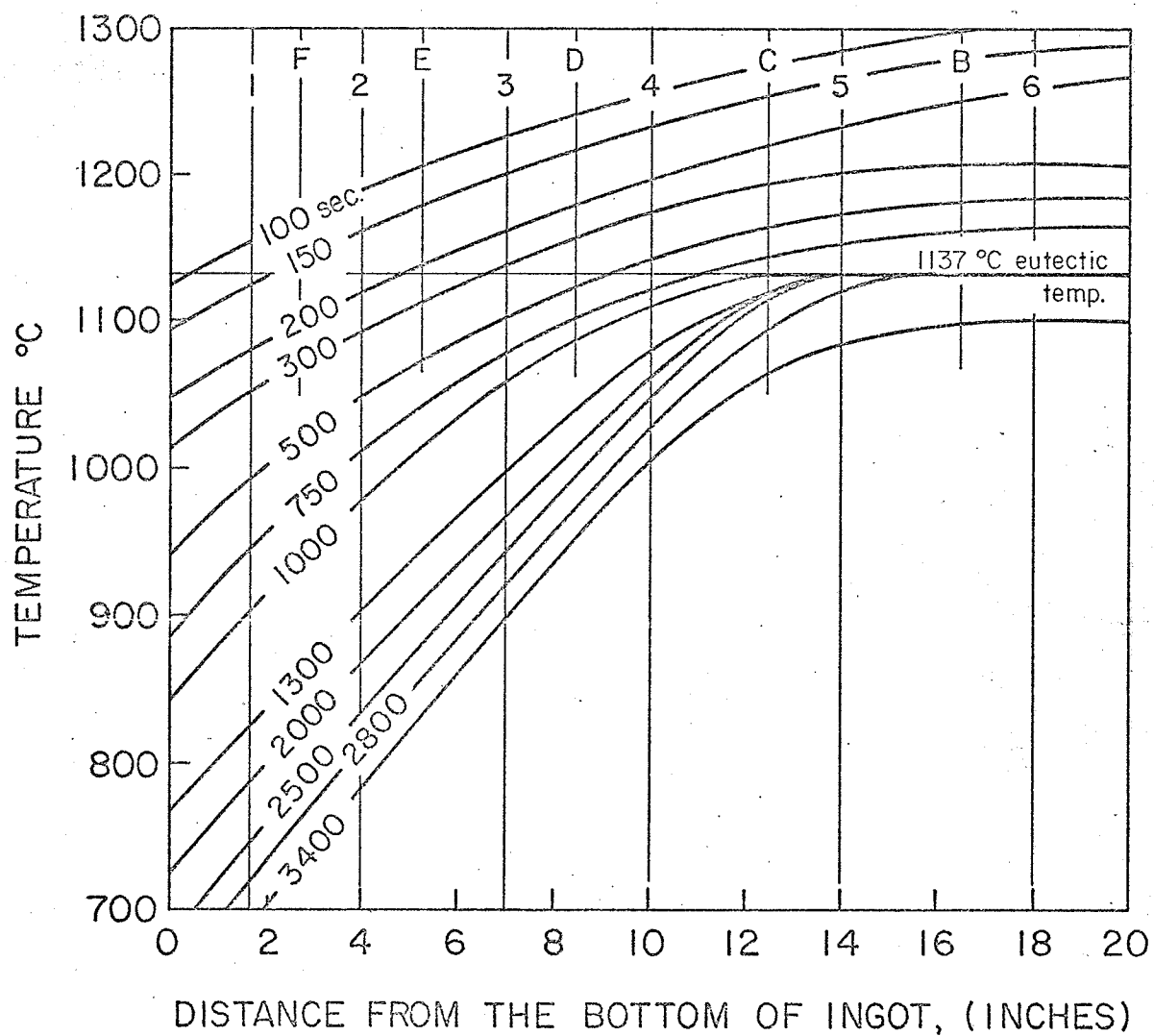


Fig. 7-b TEMPERATURE DISTRIBUTIONS IN INGOTS NO. II & III

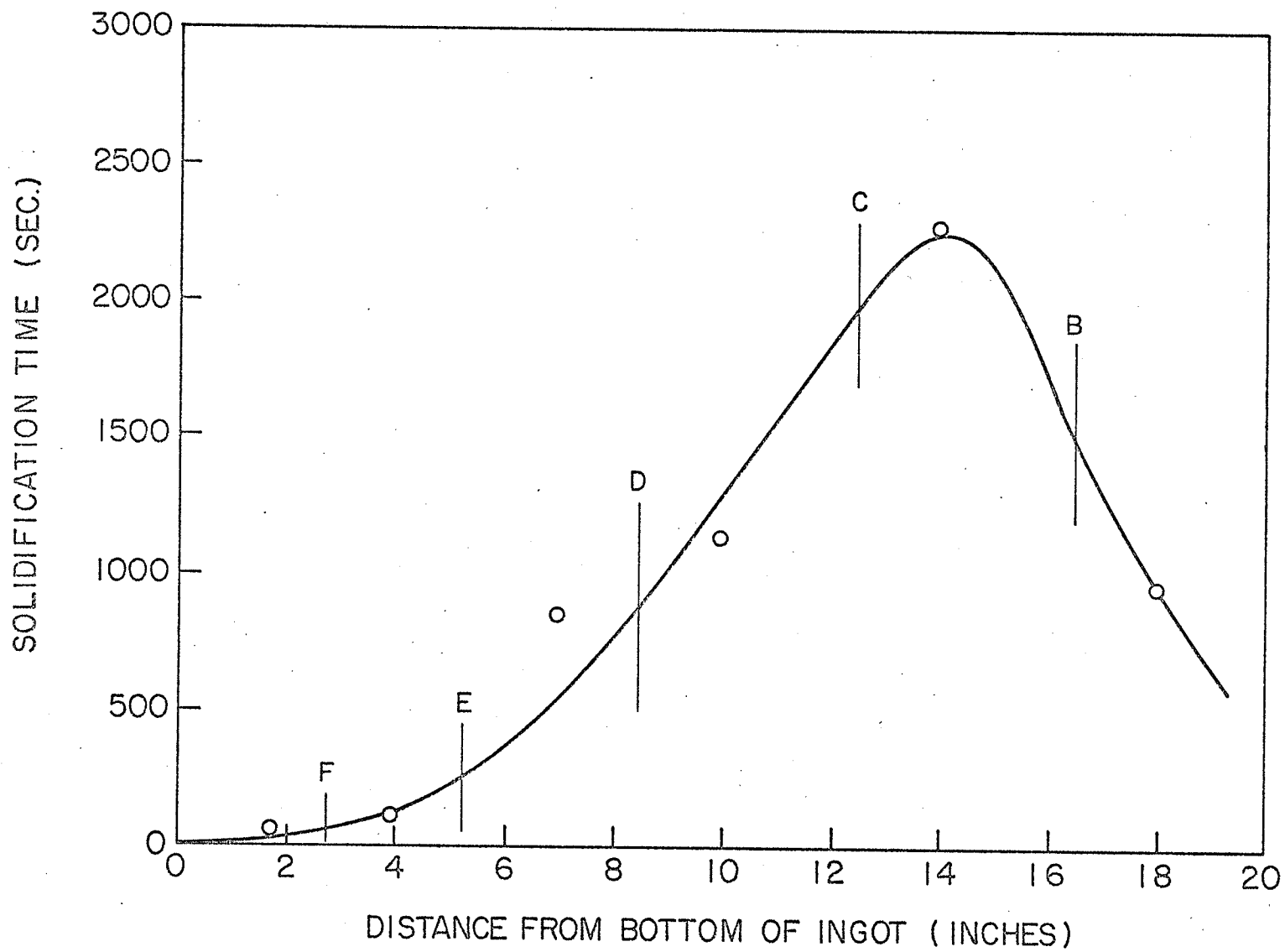


Fig. 8-a

SOLIDIFICATION TIME ALONG THE LENGTH OF INGOT I

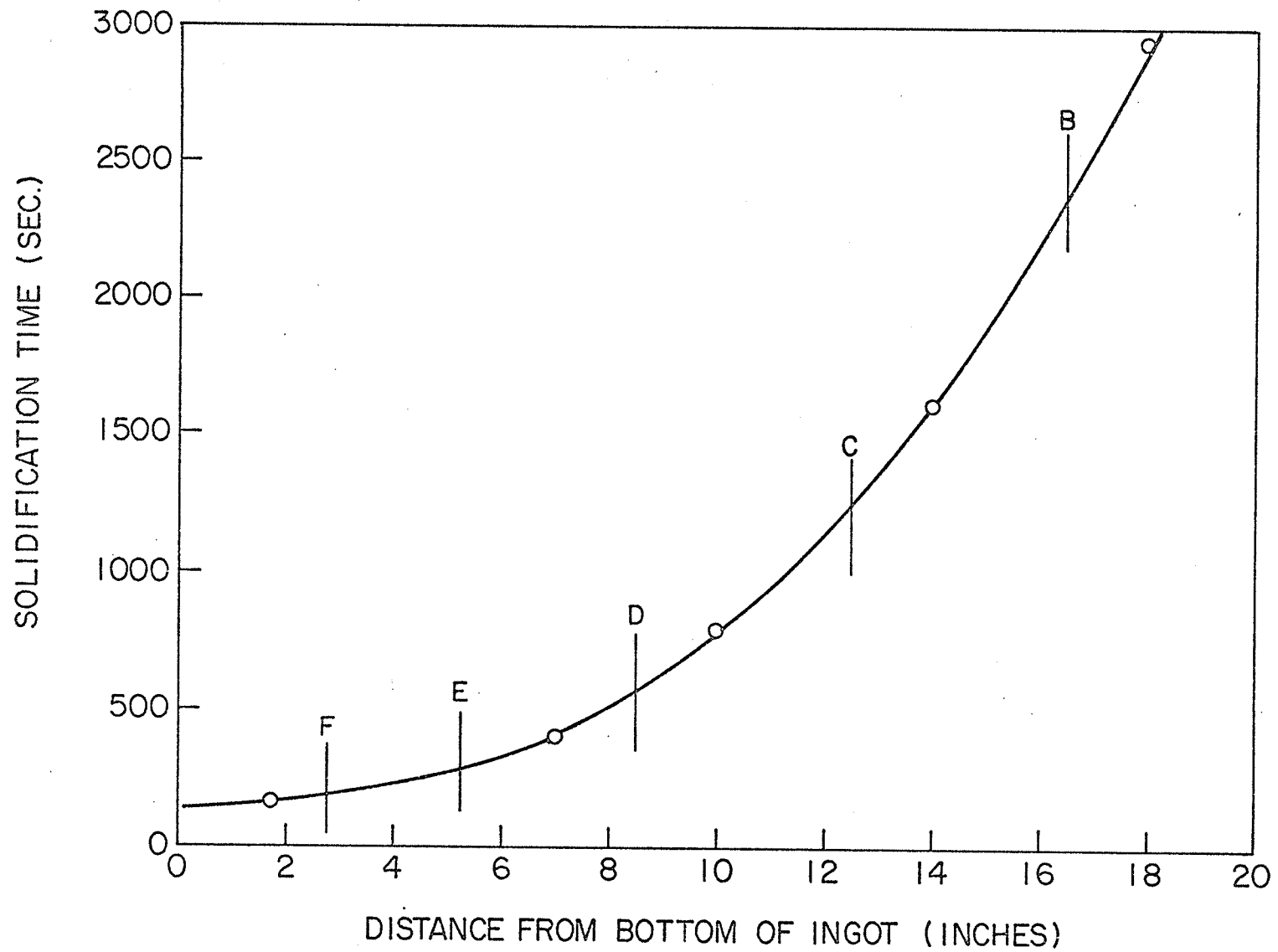


Fig.8-b SOLIDIFICATION TIME ALONG THE LENGTH OF INGOTS , II & III

In the case of bottom clevis, casting No. IV, the thermocouple arrangement was as shown in figure 5. Because of space limitation no thermocouple could be placed at section C. In order to obtain the cooling times and hence the cooling rate for all the sections to be analysed, section thicknesses were measured for every thermocouple and section size and plotted against the cooling times for 1000°C, 900°C and 700°C as shown in figure 9.

Because of smaller ingot size, complicated design and larger surface area to volume ratio, the ingot cooled very quickly and the recording equipment was unable to record the eutectic arrest. Therefore, cooling rates in °C/min instead of solidification times are used in this case. The cooling rates as obtained for sections A, C, and E are tabulated in table V.

TABLE V
COOLING RATES FOR INGOT IV

Specimen	Section Thickness inches	Time in Sec. to reach			Cooling Rate °C/min
		1000°C	900°C	700°C	
A - IV ^c	2.75	240	430	2020	32
C - IV ^c	1.75	215	355	1765	43
E - IV ^c	5.00	360	670	2400	20

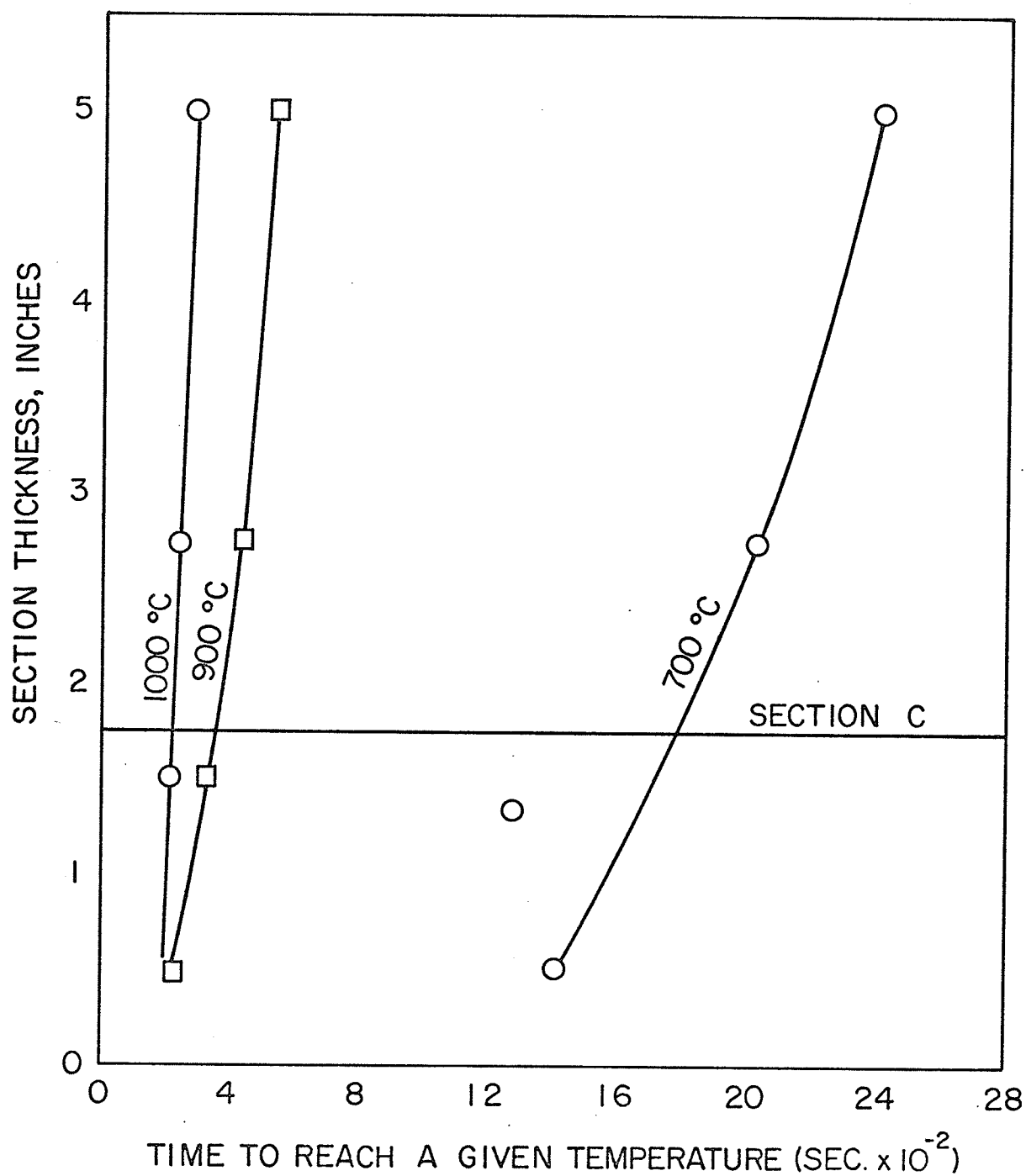


Fig. 9 TIME TO REACH 1000 °C, 900 °C & 700 °C TEMP. v/s MINIMUM SECTION THICKNESS FOR DUCTILE IRON CASTINGS NO. IV

4.2 Chemical Analysis

The results of the chemical analysis are shown in tables VI to IX for castings I, II, III and IV respectively. The elemental distribution along the ingots are also plotted in figures 10 to 14 for carbon, silicon, sulphur, manganese and magnesium respectively for the first three castings. In the case of bottom clevis, casting No. IV, the compositional variations are shown with cooling rate in figure 15. Base metal obtained before the magnesium treatment and the keel block made with the fourth ingot were also analysed and are included in the tables.

TABLE VI
CHEMICAL ANALYSIS OF INGOT NO. I

Samples from Section	% T.C.	C.E.	% Si	% S	% Mn	% Mg
B - I ^C	3.23	3.85	2.05	0.0130	0.447	0.036
C - I ^C	3.51	4.17	2.00	0.0124	0.449	0.037
D - I ^C	3.55	4.21	2.08	0.0124	0.482	0.037
E - I ^C	3.51	4.17	2.07	0.0124	0.511	0.035
F - I ^C	3.42	4.15	2.10	0.0124	0.500	0.034
Base						

TABLE VII
CHEMICAL ANALYSIS OF INGOT NO. II

Samples from Section	% T.C.	C.E.	% Si	% S	% Mn	% Mg
B - II ^C	3.18	4.07	2.68	0.019	0.32	0.028
C - II ^C	3.18	4.06	2.65	0.020	0.34	0.027
D - II ^C	3.03	3.94	2.73	0.018	0.30	0.025
E - II ^C	3.25	4.15	2.70	0.021	0.36	0.029
F - II ^C	3.48	4.38	2.71	0.022	0.38	0.025
Base	3.66	4.28	1.87	0.028	0.30	0.007

TABLE VIII

CHEMICAL ANALYSIS OF INGOT NO. III

Samples from Section	% T.C.	C.E.	% Si	% S	% Mn	% Mg
B - III ^C	2.04	3.06	3.28	0.022	0.30	0.040
C - III ^C	2.03	3.05	3.29	0.022	0.30	0.039
D - III ^C	2.62	3.63	3.27	0.023	0.31	0.039
E - III ^C	2.21	3.23	3.29	0.023	0.31	0.038
F - III ^C	2.93	3.95	3.29	0.021	0.31	0.034
Base						

TABLE IX

CHEMICAL ANALYSIS OF INGOT NO. IV

Samples from Section	% T.C.	C.E.	% Si	% S	% Mn	% Mg
A - IV ^C	3.12	4.22	3.54	0.016	0.31	0.034
C - IV ^C	2.69	3.80	3.57	0.016	0.31	0.030
E - IV ^C	3.01	4.11	3.54	0.016	0.31	0.032
Keel Block	2.97	4.07	3.56	0.013	0.31	0.031
Base	3.71	4.48	2.49	0.031	0.30	0.003

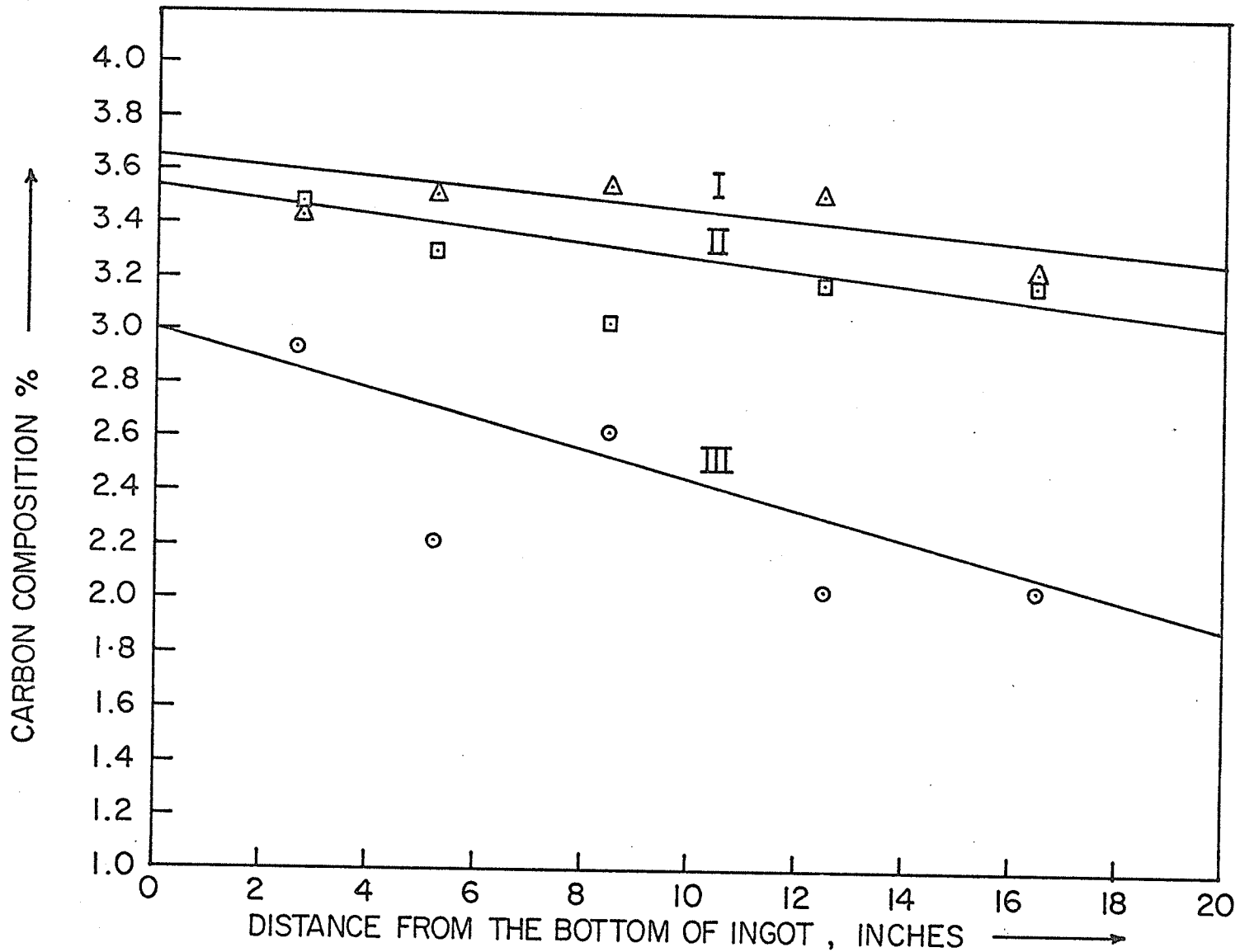


FIG.-10. CARBON DISTRIBUTION ALONG INGOTS NO. I, II and III.

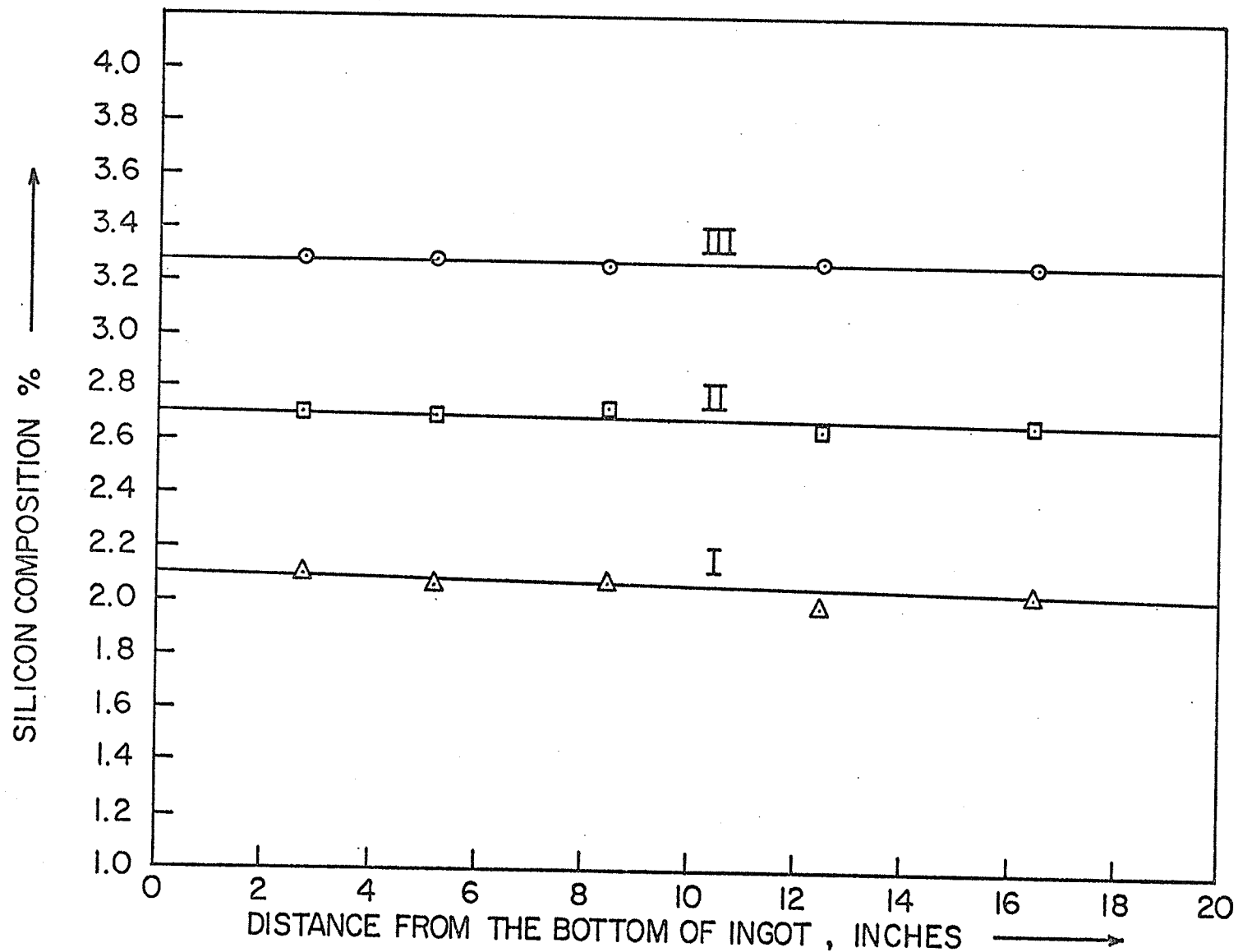


FIG.-II. SILICON DISTRIBUTION ALONG INGOTS NO. I, II and III.

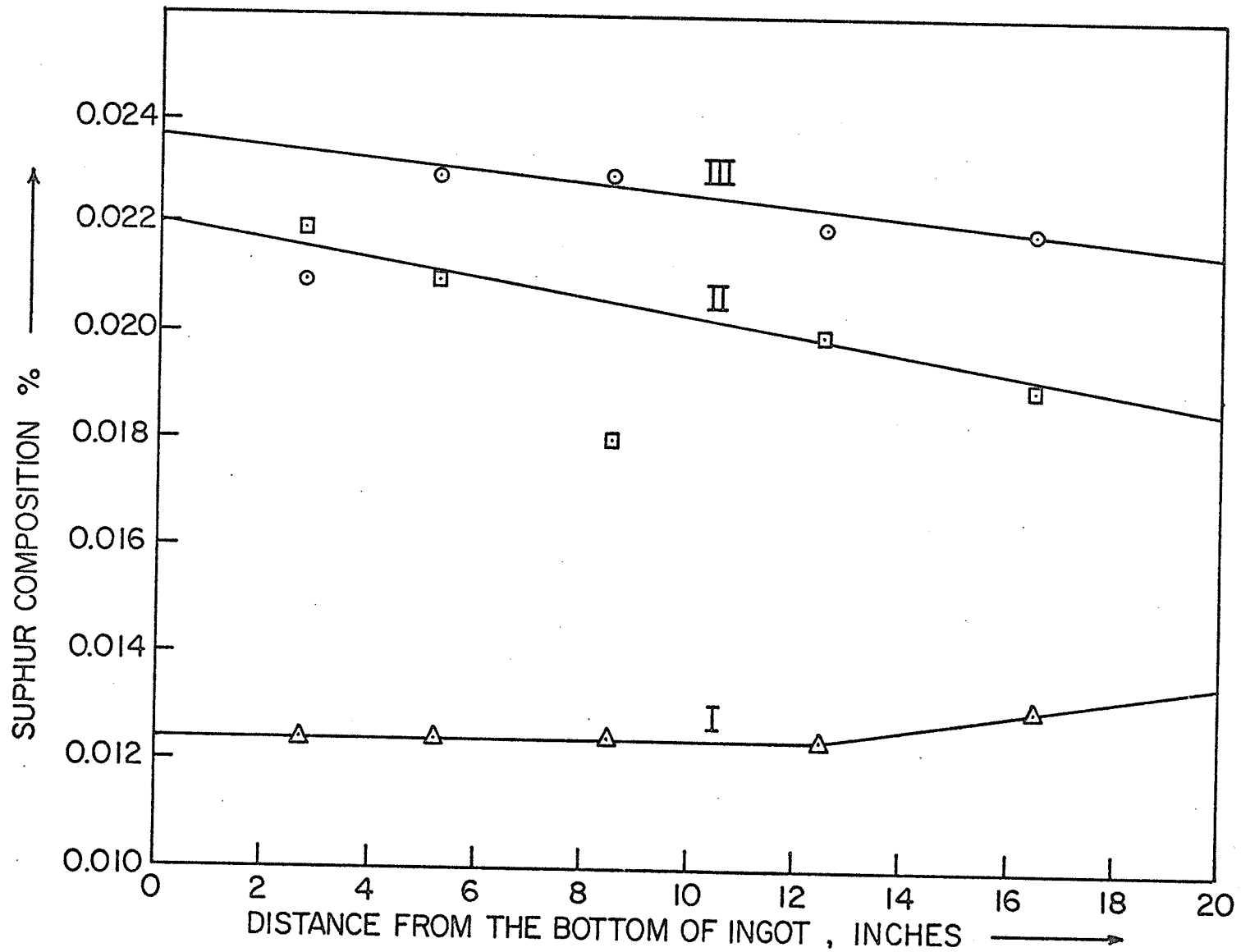


FIG. - 12. SULPHUR DISTRIBUTION ALONG INGOTS NO. I, II and III.

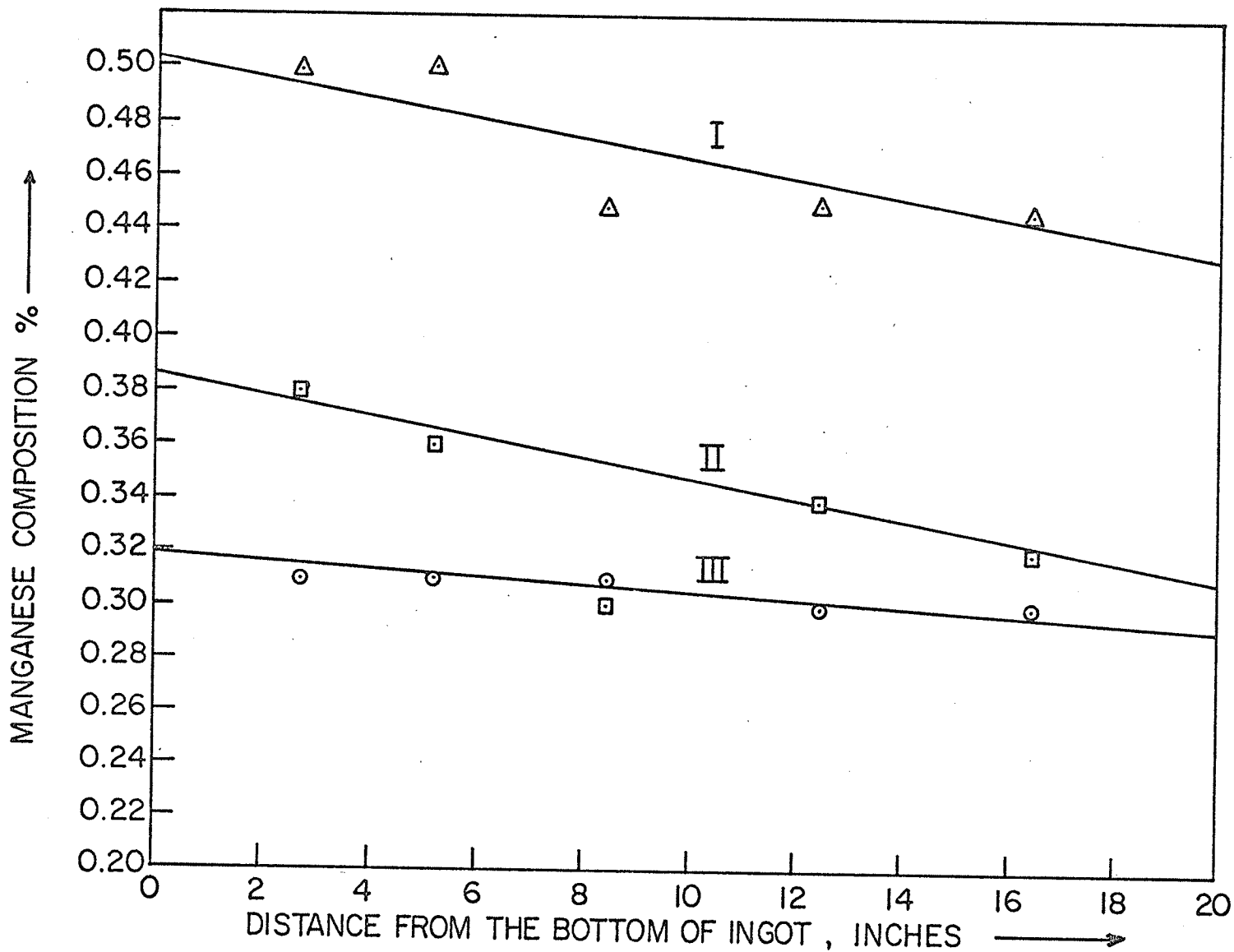


FIG. - 13. MANGANESE DISTRIBUTION ALONG INGOTS NO. I, II and III.

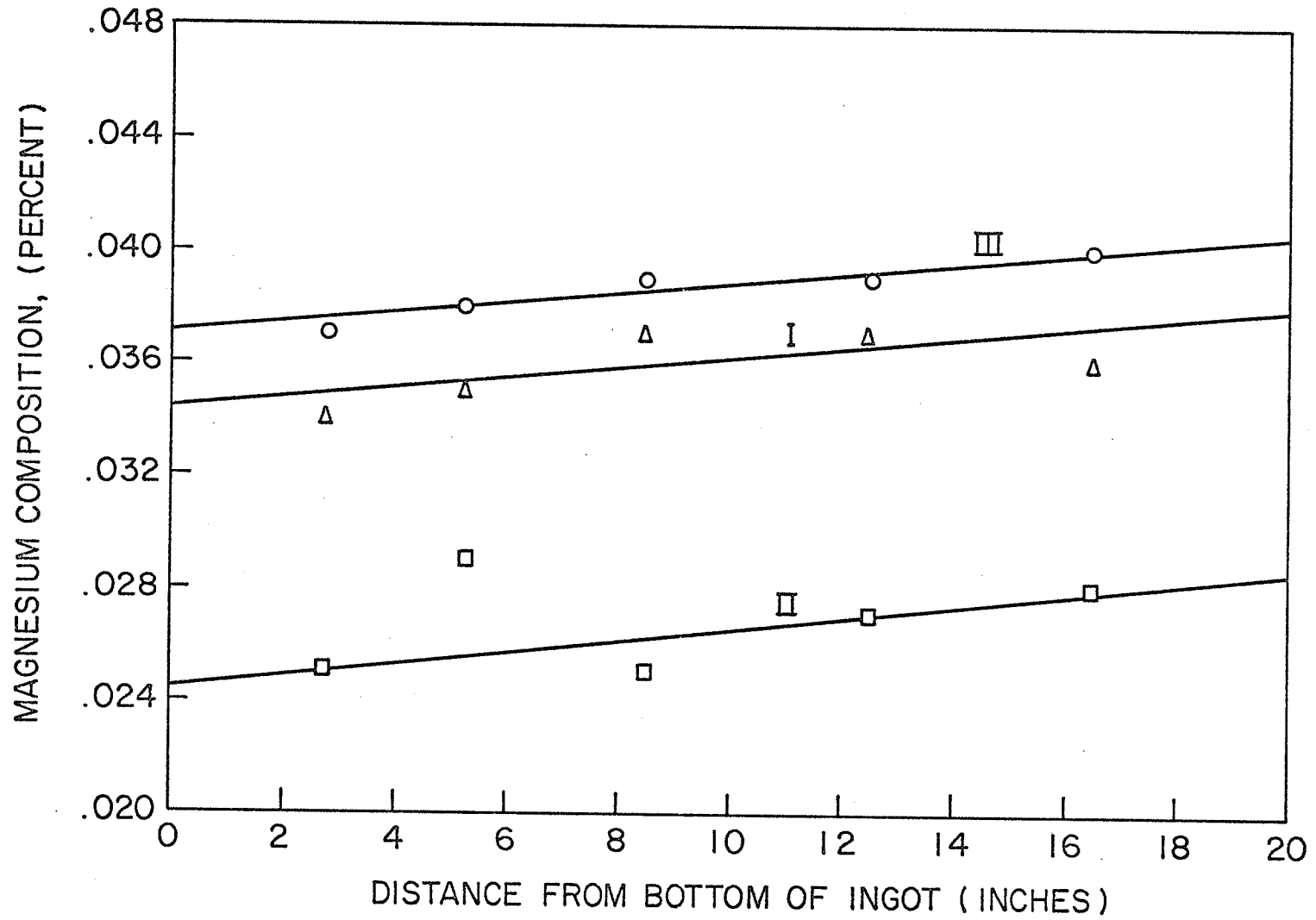


Fig. 14 MAGNESIUM DISTRIBUTION ALONG INGOTS, I, II, III

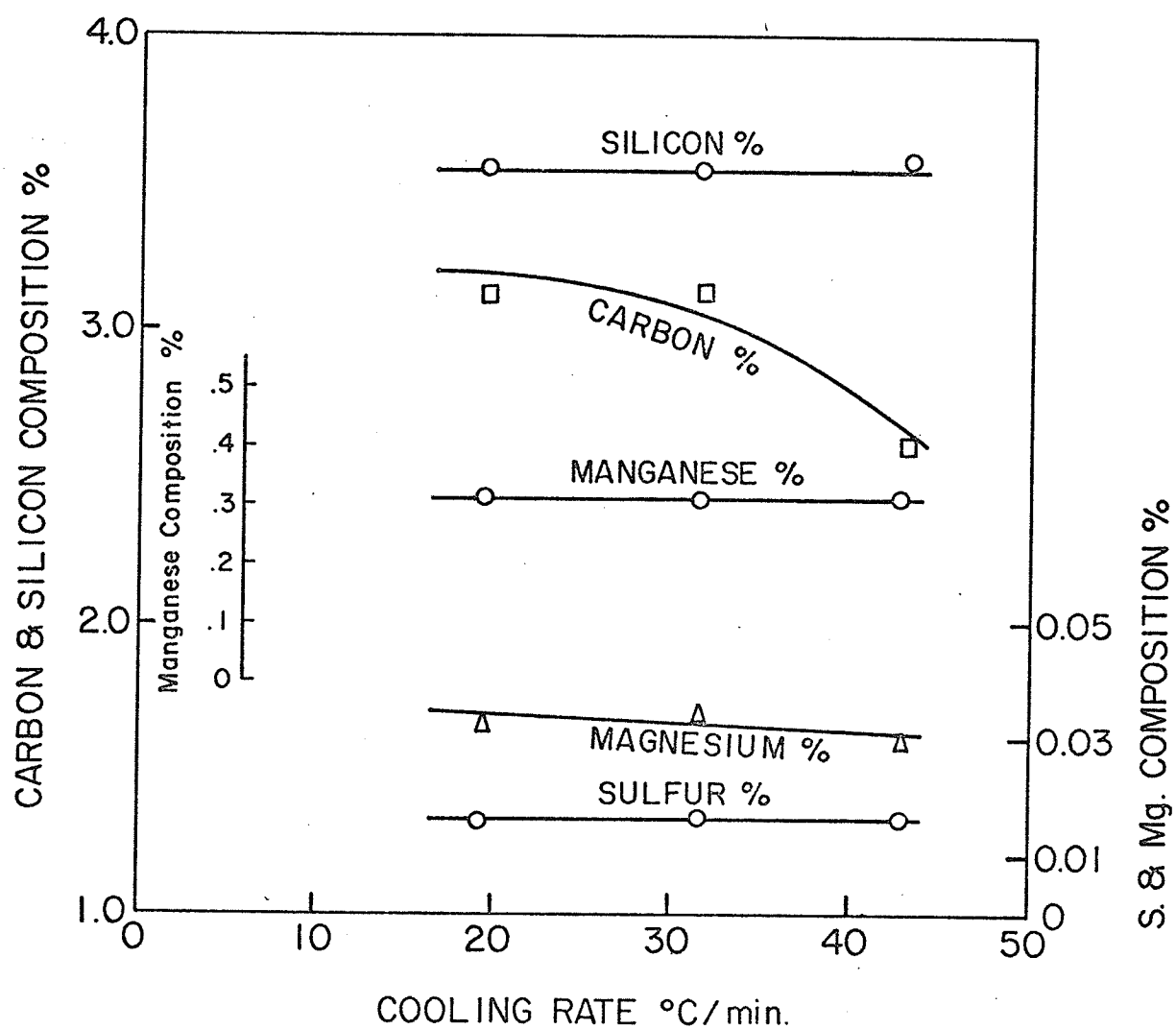


Fig.15 COMPOSITION VARIATION WITH COOLING RATE IN CASTING NO. IV BOTTOM CLEVIS

4.3 Metallographic Observations

Figures 16 to 19 show the microstructures of castings 1 to 4 respectively. In the first three cases B, C, D, E and F represent the sections as were shown in figure 6, whereas in figure 19 the sections are represented as A, C, and E (figure 5).

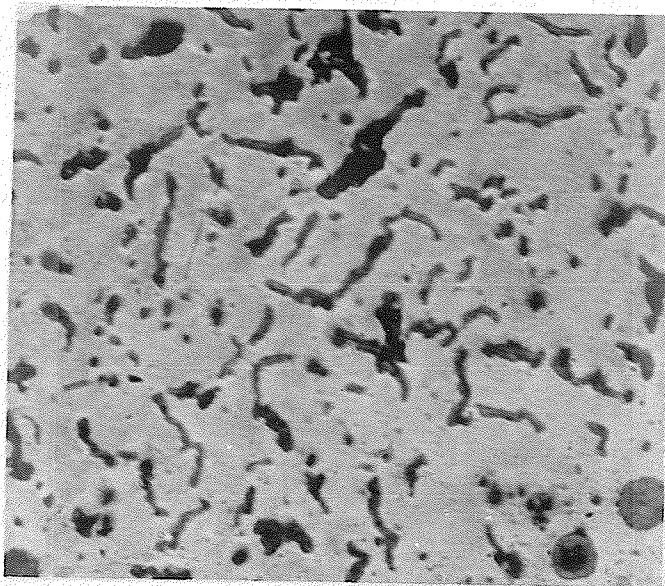


Fig. 16-B Microstructure of normalized ductile iron casting No. 1 Section B. x 100, 3% Nital etched.

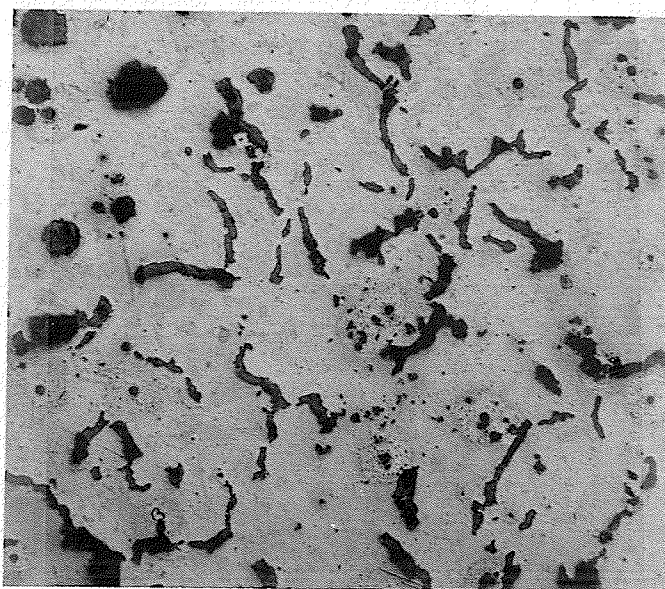


Fig. 16-C Microstructure of normalized ductile iron casting No. 1 Section C. x 100, 3% Nital etched.

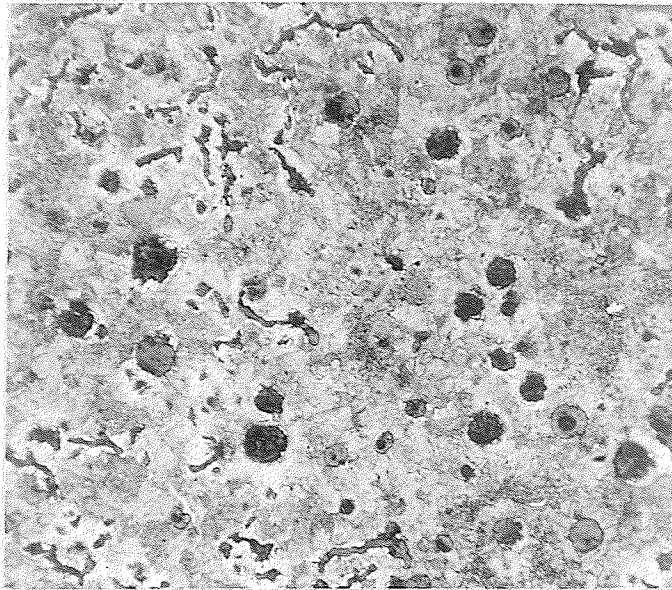


Fig. 16-D Microstructure of normalized ductile iron casting No. 1 Section D. x 100, 3% Nital etched.

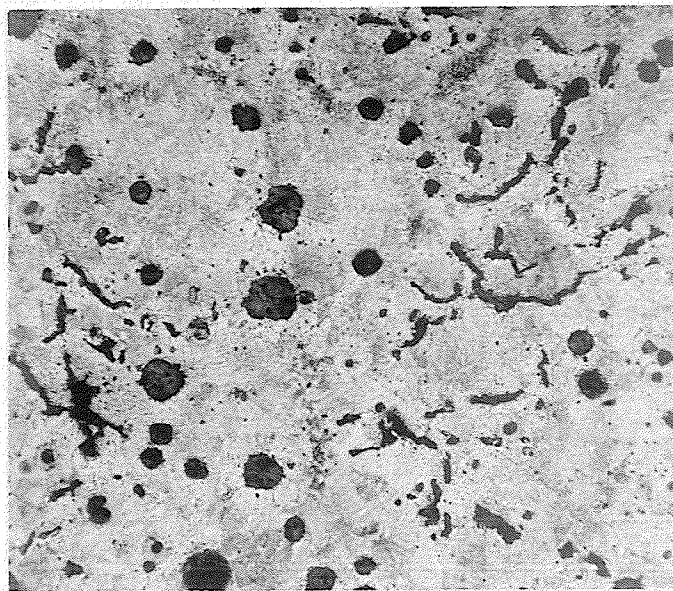


Fig. 16-E Microstructure of normalized ductile iron casting No. 1 Section E. x 100, 3% Nital etched.

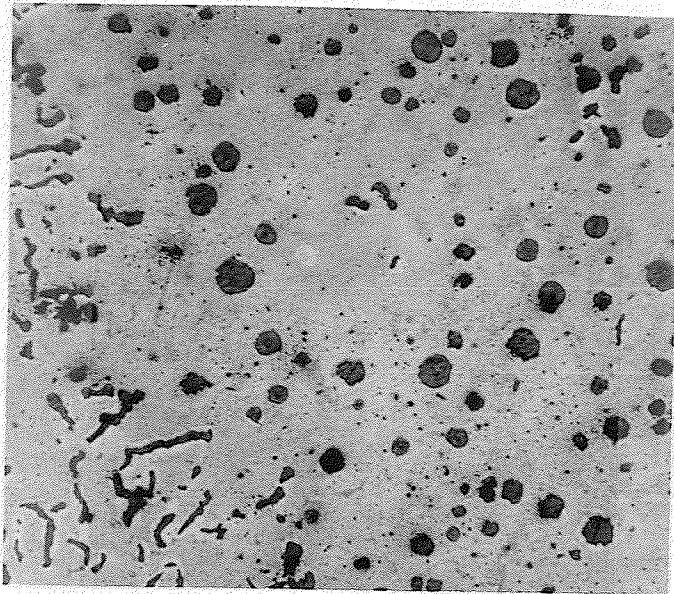


Fig. 16-F Microstructure of normalized ductile iron casting No. 1 Section F. x 100, 3% Nital etched.



Fig. 17-B Microstructure of as-cast ductile iron casting No. 2 Section B. x 100, 3% Nital etched.

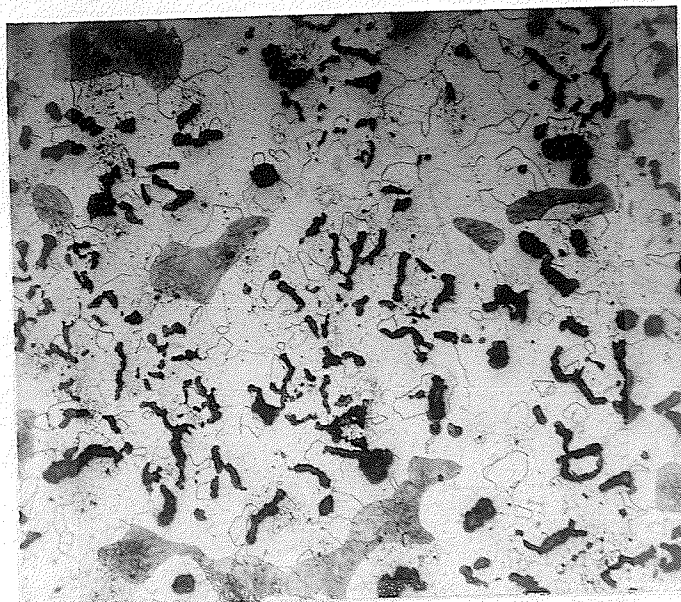


Fig. 17-C Microstructure of as-cast ductile iron casting No. 2 Section C. x 100, 3% Nital etched.

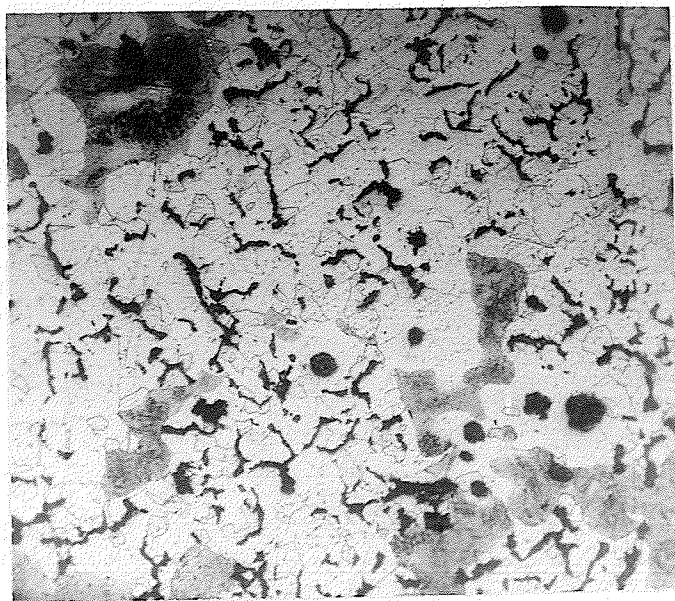


Fig. 17-D Microstructure of as-cast ductile iron casting No. 2 Section D. x 100, 3% Nital etched.

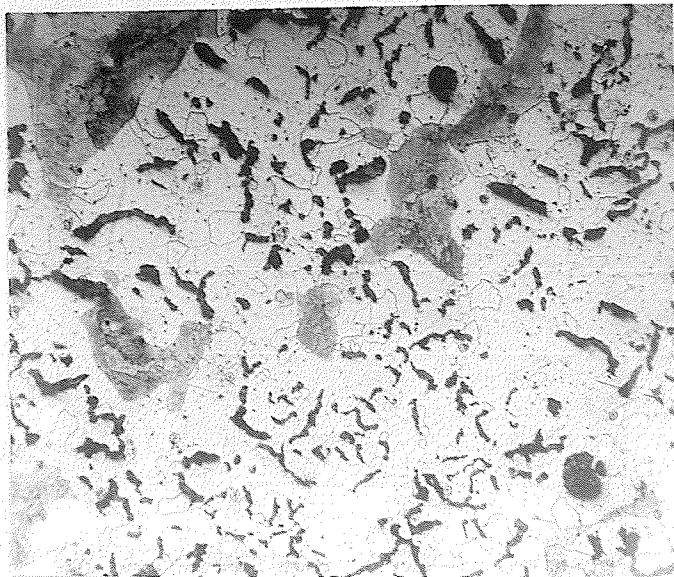


Fig. 17-E Microstructure of as-cast ductile iron casting No. 2 Section E. x 100, 3% Nital etched.

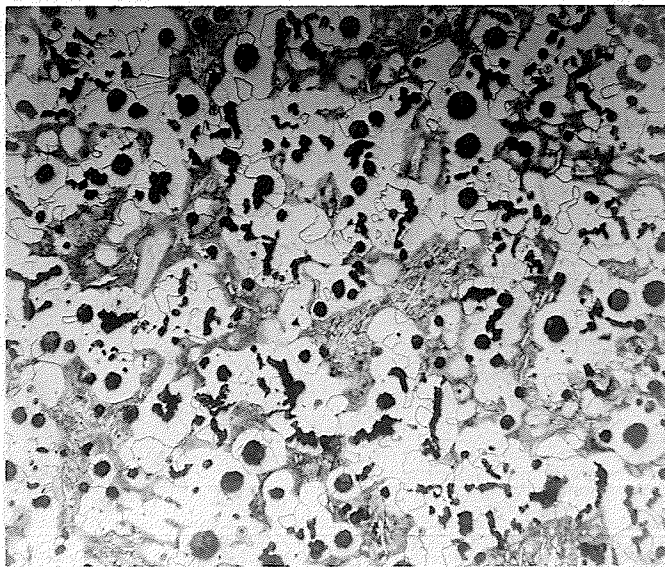


Fig. 17-F Microstructure of as-cast ductile iron casting No. 2 Section F. x 100, 3% Nital etched.

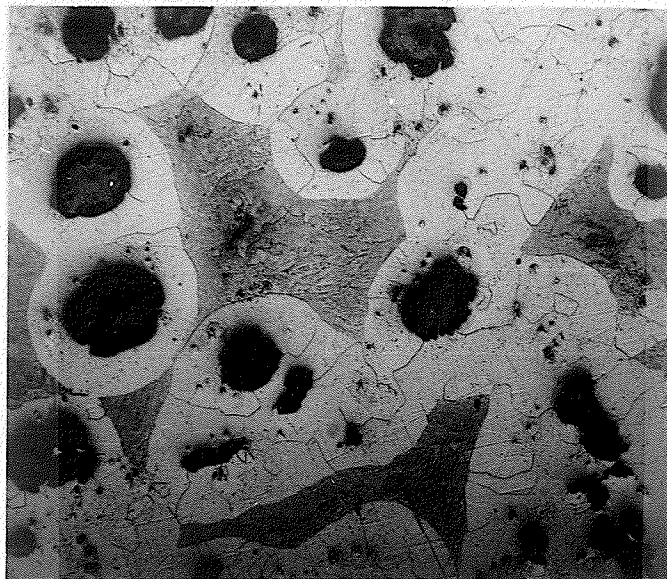


Fig. 18-B Microstructure of as-cast ductile iron casting No. 3 Section B. x 100, 3% Nital etched.

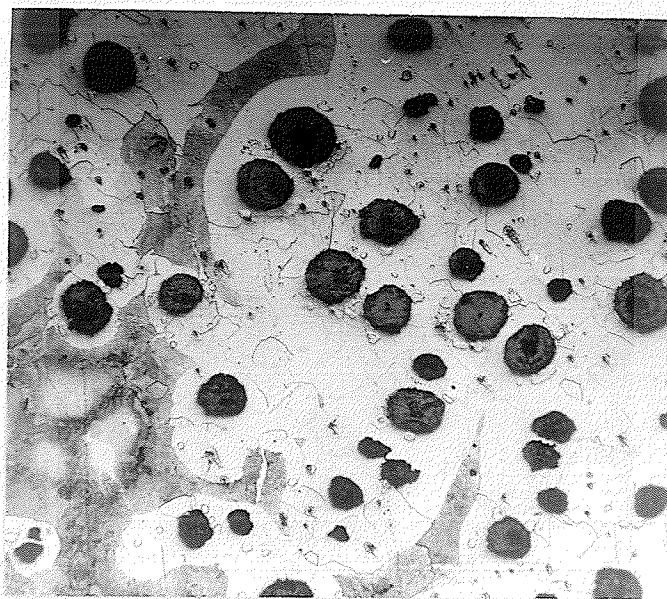


Fig. 18-C Microstructure of as-cast ductile iron casting No. 3 Section C. x 100, 3% Nital etched.

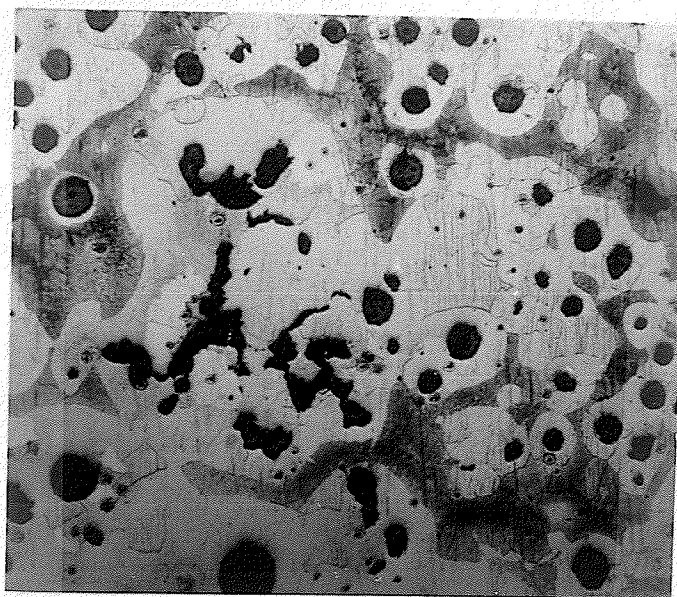


Fig. 18-D Microstructure of as-cast ductile iron casting No. 3 Section D. x 100, 3% Nital etched.

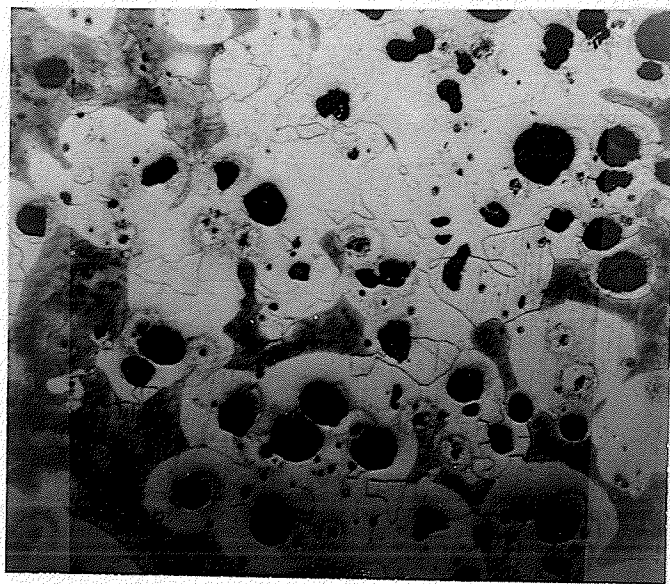


Fig. 18-E Microstructure of as-cast ductile iron casting No. 3 Section E. x 100, 3% Nital etched.

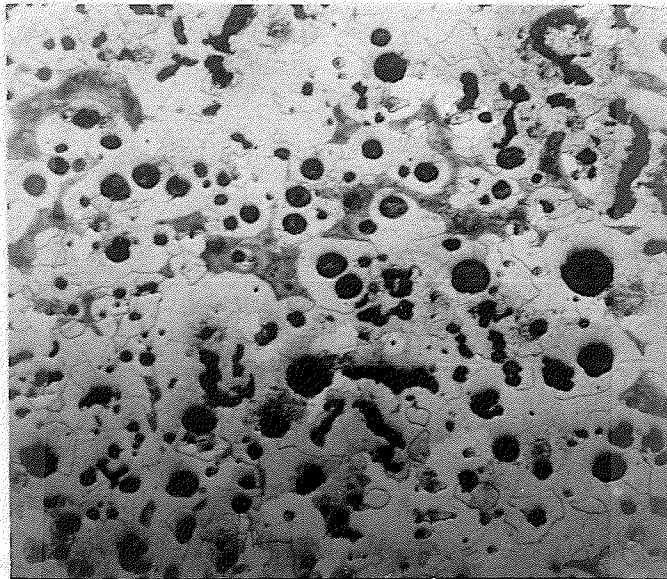


Fig. 18-F Microstructure of as-cast ductile iron casting No. 3 Section F. x 100, 3% Nital etched.

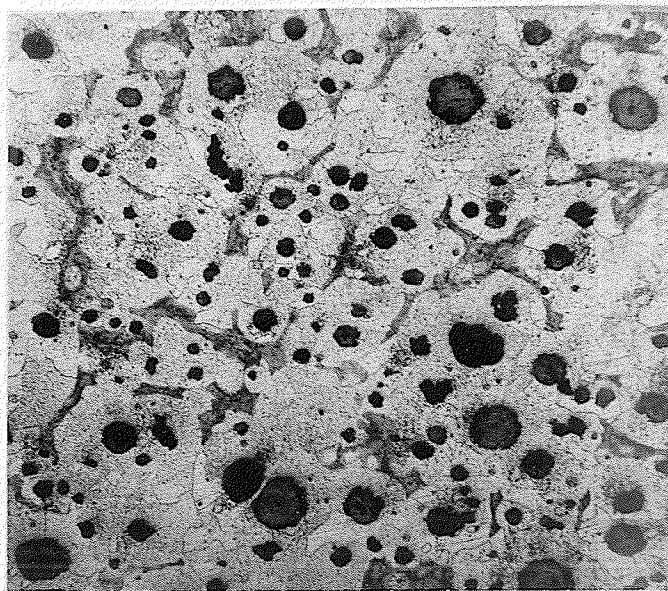


Fig. 19-A Microstructure of as-cast ductile iron casting No. 4 Section A. x 100, 3% Nital etched.

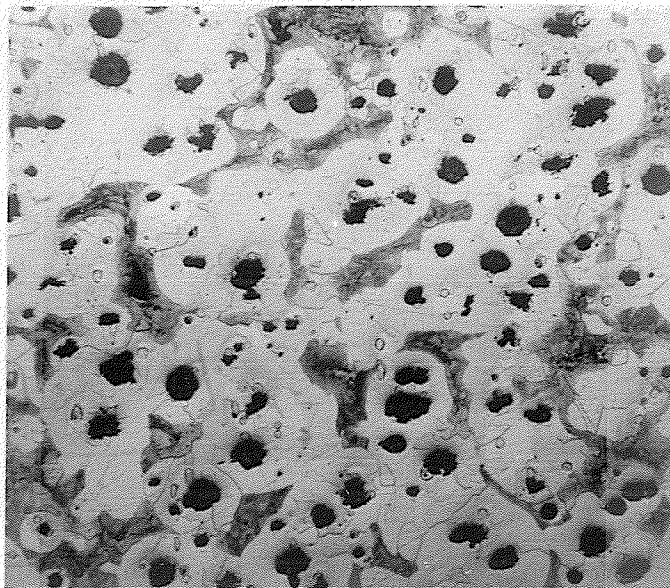


Fig. 19-C Microstructure of as-cast ductile iron casting No. 4 Section C. x 100, 3% Nital etched.

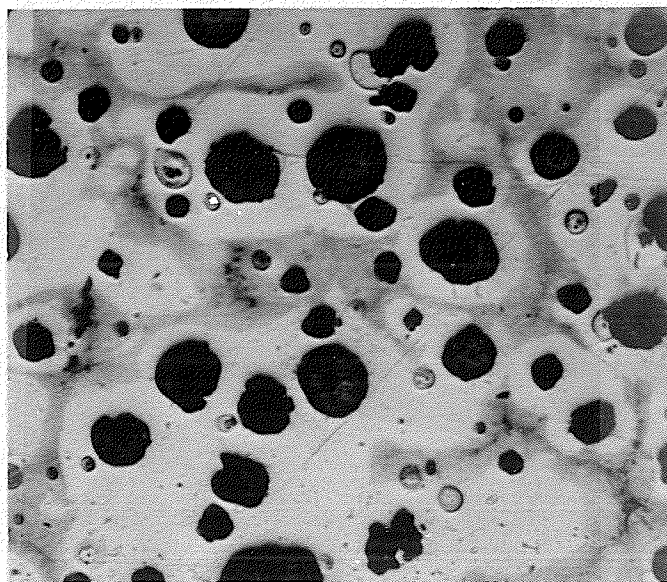


Fig. 19-E Microstructure of as-cast ductile iron casting No. 4 Section E. x 100, 3% Nital etched.

4.4 Tensile Properties

Figures 20 to 23 represent the results of tensile tests on different sections of the four castings as plotted against solidification times and cooling rates. It is of interest to note the effect of solidification times and cooling rates on the microstructure, which in turn had a marked effect on the mechanical properties of the metal as is obvious from the above mentioned figures. This effect is discussed in greater detail in the next chapter. It should be remembered that specimens from ingot I were given a normalizing heat treatment while specimens from the remaining ingots were tested in the as-cast condition.

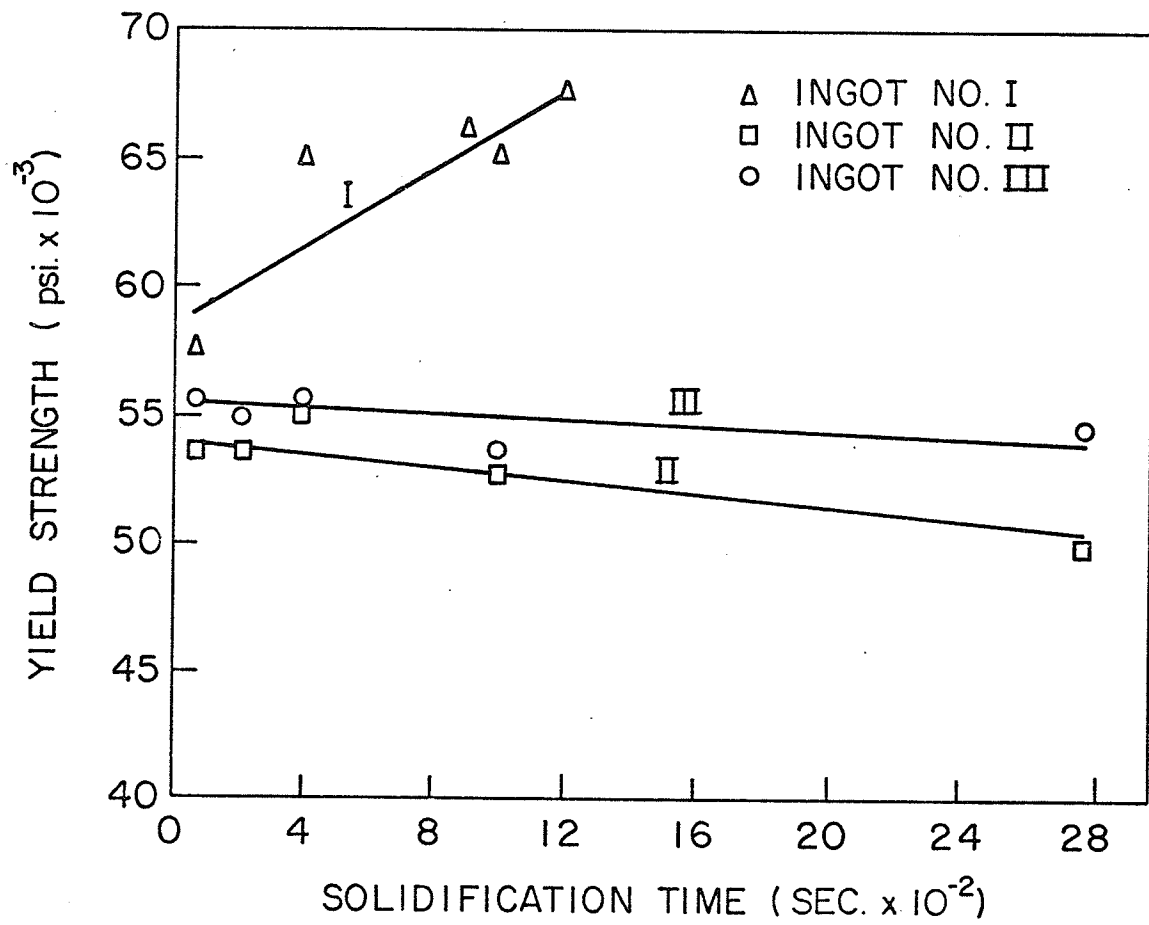


Fig.20 YIELD STRENGTH vs. SOLIDIFICATION TIME FOR INGOTS I, II, III

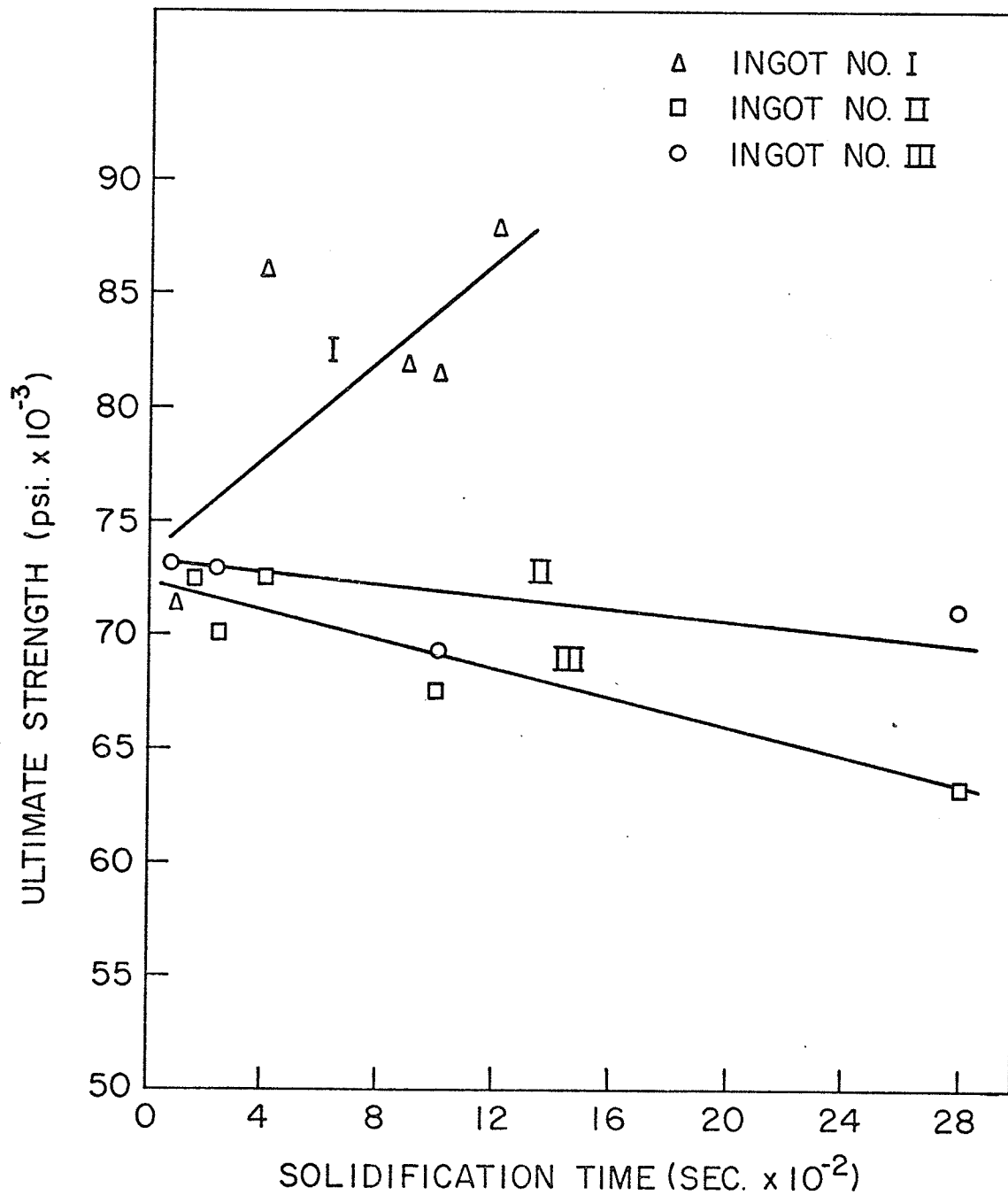


Fig.2I TENSILE STRENGTH vs. SOLIDIFICATION TIME FOR INGOTS I, II, III

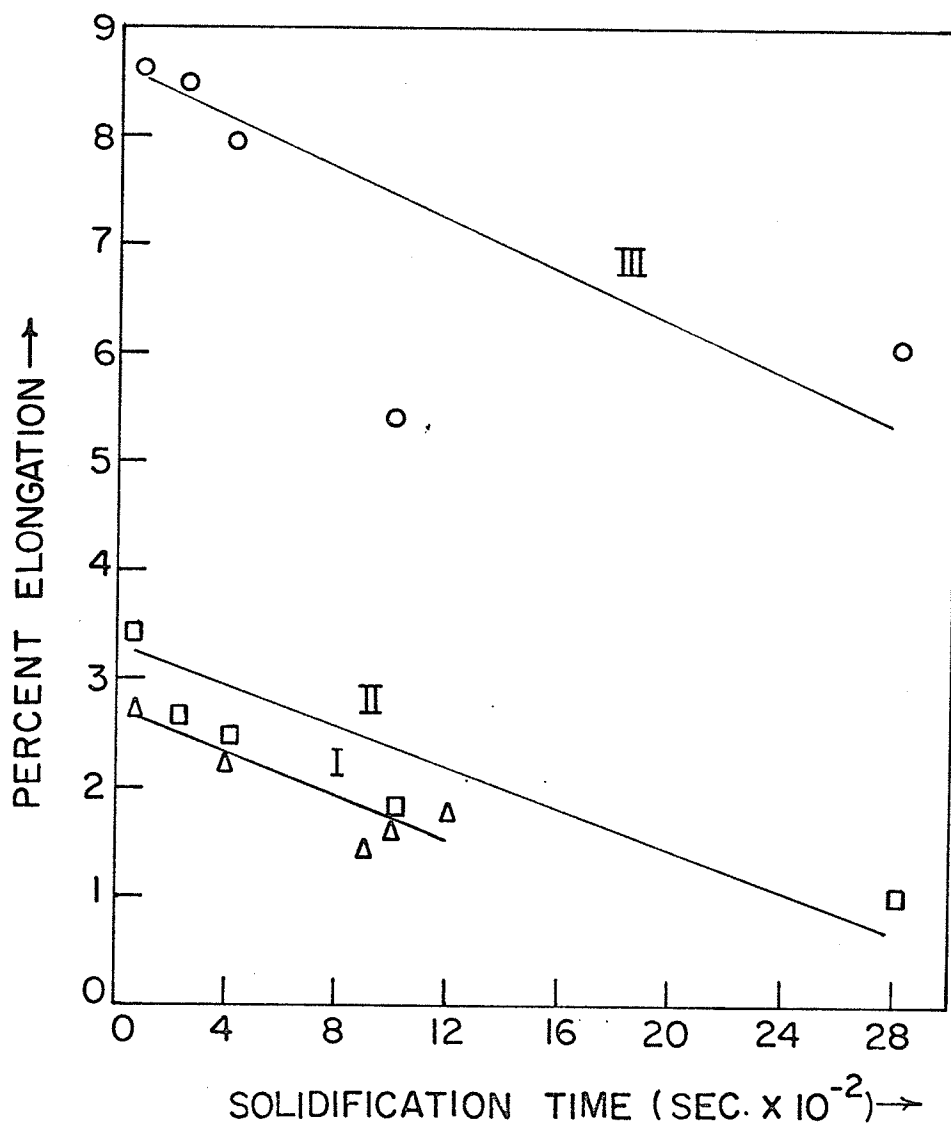


Fig. 22 % ELONGATION v/s SOLIDIFICATION TIME
FOR INGOTS NO. I, II & III

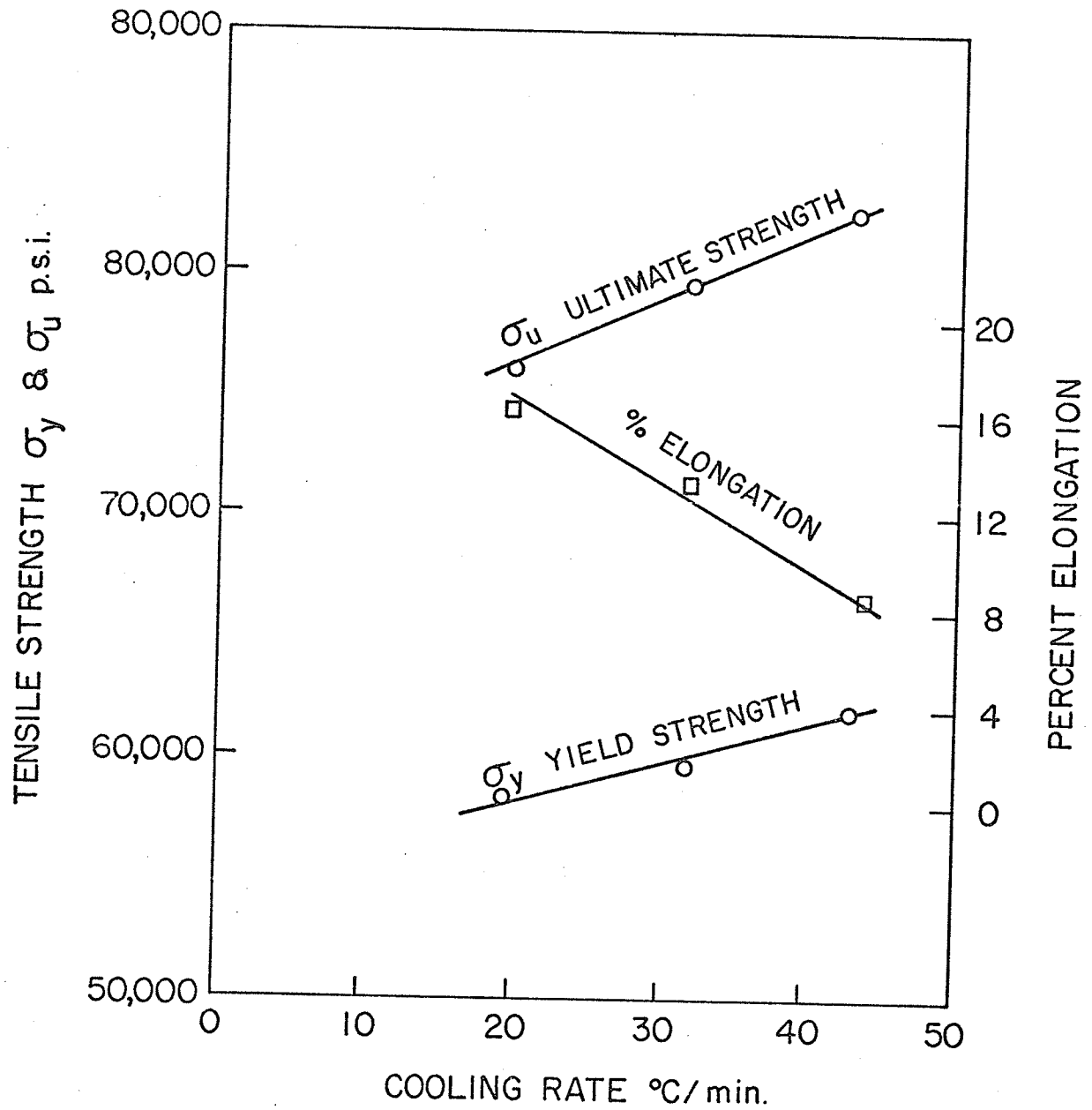


Fig. 23 MECHANICAL PROPERTIES OF CASTING NO. IV
BOTTOM CLEVIS

5. DISCUSSION OF RESULTS

5.1 Effect of Charge Material

Selection of the right amount of charge material is the first step to obtain an economically sound casting of required grade and properties. The factors considered in selection are the cost of charge material, the type of furnace lining and the melt size, etc. The greater use of scrap steel for the making of ductile iron, although keeping the charge cost down, makes the control of chemical composition difficult. The use of pig iron is more expensive but helps in obtaining the required grade of ductile iron.

Ductile iron charge also depends on the type or basicity of the furnace. For example, pig iron is necessary to dilute impurities, especially sulphur, in the charge in an acid cupola, whereas in a basic type of furnace very little or no pig iron is used in some cases. De-sulphurization is also highly recommended and a greater amount of magnesium is required for acid cupola melting. Carbon content is usually higher in basic cupola melting which, if not controlled, results in graphite floatation. An item not generally recognized is that in a basic cupola up to about 40 to 50 percent of the charged silicon is lost during the melting operation²³ as compared to only 10% in acidic melting.⁴

Although the charge cost for a basic cupola is lower than that of an acidic one it is preferred only by large foundries because of its higher refractory cost. The cupola lining cost per melt ton is 4 to 5

times greater for a ductile iron basic cupola operation than an acidic lined one. The smaller industries still are more inclined to use acid cupolas because they are more economical to use for small melts. Coke consumption is also relatively high in a basic cupola.

The effect of the two different charge composition and alloying elements listed in table III is obvious from the results of the chemical analysis and comparison of the graphite morphology of the four ingots. The use of almost 50% scrap steel which was diluted by only 10% of pig iron in the first case affected the graphite morphology of ingots I and II. Higher impurity content of steel caused the graphite nodules to degenerate into flakes. The use of better balanced charge in the second case resulted in nodular graphite structure.

The ductile iron melt was prepared in an acidic furnace which as mentioned above, requires a much closer control of chemical composition. The control of chemical composition in this case was limited to the determination of carbon and carbon-equivalent only, although a complete chemical analysis of the base metal prior to magnesium treatment was required, particularly in the case of the first two castings because of the use of a higher percentage of steel scrap. The average carbon-equivalent of 4.08 for the first ingot and 4.06 for the second ingot is very low to obtain a good ductile iron.

5.2 Solidification Time and the Effect of Section Size

Almost all the properties of ductile irons are dependent on the section size and cooling rate of the casting. Figure 7 (a and b) shows the effect of section size on the solidification time of the three experimental wedge-shaped castings. The wedge thickness varied from zero inches at the bottom of the ingot to 6 inches at the top. The time of solidification increased in the same way with the section size. The cooling rate affects the tendency of cast iron to form iron carbide or graphite during solidification. The more rapid solidification does not give graphite enough time to form and therefore increases the carbide forming tendency. Since carbon and silicon are the only two elements which strongly promote a carbide free as cast structure, a high carbon equivalent is selected for uniformly thin casting. The danger of graphite floatation exists with large differences in section size, and heat treatment with all its disadvantages is almost unavoidable in such cases. The main disadvantages of heat treatment are difficulty in cleaning and getting exact dimensional accuracy. The amount of elements like Mn and Mg, etc. which promote carbides also has to be kept low in thin section castings.

Inoculation in ductile iron is a more common method of reducing the danger of as-cast carbides. Ferro-silicon inoculants were used in both the charges for our ductile iron to avoid the formation of carbides.

5.3 The Chemical Composition

The differences in the chemical composition of the four ingots affected the microstructure and mechanical properties of the ductile iron. Tables VIII and IX for the third and fourth ingots respectively represents a better balanced chemical composition as compared to tables VI and VII for ingots I and II respectively.

Carbon being the main constituent of cast iron in general and silicon being the second important element for the production of a carbide-free as-cast structure, has to be relatively higher in percentage as compared to gray iron. Carbon-equivalent [C.E. = %T.C. + 0.31% Si] of 4.3 near eutectic is most favourable for obtaining a sound and cheap casting. The analysis done on the castings shows carbon-equivalent to be low for ingots I, II and III. Carbon composition was low throughout the four ingots, particularly in ingots II and III. The carbon deficiency was somewhat compensated for by high silicon composition in ingots III and IV, but in ingots I and II the iron turned out to be more like gray iron rather than ductile. Silicon deficiency in the first ingot and both carbon and silicon deficiency in the second ingot caused the graphite morphology to change from nodular to flaky. There was 0.2 to 0.75 % carbon loss during the magnesium treatment which should have been considered in the charge calculations. The silicon content on the other hand was raised by approximately 1.0%.

The increase in the total silicon content from 2.0% for the first ingot to 3.57% for the fourth ingot (tables VI to IX) was observed to

increase the as-cast ferritic matrix structure (figures 16 to 19). This was also demonstrated by an increase in percent elongation with increasing silicon composition (figures 22 and 23). The elongations observed were 2.7% maximum for ingot I, 3.5% maximum for ingot II, 8.6% maximum for ingot III and 16.3% maximum for ingot IV.

Free sulphur which obstructs the formation and growth of graphite nodules was generally below the maximum allowable mark and most probably had no influence on the graphite morphology or matrix structure of the metal. Also, in ingot I the amount of manganese was about 0.08% higher than the amount which would balance free sulphur present as indicated by equation (4). Magnesium, the most important element for spheroidizing, was present in adequate amounts in all ingots with the exception of the second ingot in which it was low.

No significant segregation of elements present in the iron was observed along the length of the ingot (figures 10 to 15). The maximum concentration difference observed was in the case of carbon in the third ingot. It varied from 2.04% at section B to 2.93% at section F. With the exception of magnesium (figure 14) and silicon (figure 11) all the elements were at a higher concentration in the regions that solidified earlier, section F, than in those that solidified later, section B. Silicon showed no or very slight concentration difference along the length of the ingot, whereas the magnesium concentration decreased with decrease in time of solidification.

5.4 Metallography

The graphite morphology for the first two ingots were more flaky than nodular because of unbalanced chemical composition and poorer quality control. Comparatively greater numbers of round nodules were observed at higher cooling rates, which diminished in number and had degenerated graphite shape as the cooling rate decreased. Well shaped graphite nodules were readily formed in the third and fourth ingots (figures 18 and 19) which had better quality control. Chunky and irregular forms of graphite were observed in all the four ingots, but they were rare in the last two ingots. Figures 18-b, 18-d, 18-f and 19-c show a few degenerated graphite nodules.

The increase in the silicon (figures 11 and 15) and magnesium (figures 14 and 15) in the four ingots seems to considerably improve the graphite morphology from flaky to nodular.

In the as-cast condition, ingot I was mostly pearlitic with traces of ferrite around the graphite nodules. The samples from the ingot were normalized to give a very fine almost completely pearlitic matrix structure.

With the increase in the silicon content of the iron, more ferrite occurred in the as-cast microstructure. The iron contained from 20 to 60% ferrite (volume fraction) in the as-cast condition. Traces of pearlite, 10 to 30%, were also present in the II, III and IV ingots. The volume fraction was determined by using a point counting method. A transparent

grid was placed over the photomicrograph and the number of grid intersections falling over the ferrite, or pearlite or graphite were counted separately and divided by the total number of grid intersections to give area or volume fractions.

The nodular graphite morphology did not show a very strong dependence on the cooling rate, but some difference was observed in the nodule to flake graphite ratio in the case of the first two ingots which revealed a microstructure which was more like gray iron rather than ductile (figures 16 and 17). The nodule to flake ratio increased with increasing cooling rate. The nodule to flake ratio was 0.03 and 0.05 at section B in ingots I and II respectively and were 1.0 and 0.5 at section F for ingots I and II.

The most observable effect of cooling rates on the graphite structure was the expected one; at higher cooling rate the graphite nodules and flakes were relatively much finer and were present in much larger quantities than at lower cooling rates.

5.5 The Mechanical Properties

The mechanical properties of metals are a consequence of their internal structure. The degree of dependence upon the microstructure varies from property to property. The grain size, shape, and orientation plus the difference in phase amounts and local segregation all influence in some form or degree the properties of the metal. For example, the decrease in grain-size produces an increase in resistance to plastic

deformation. If the deformation is occurring by slip, then the probability for slip interference is a function of grain boundary area and an inverse function of the grain dimension.²⁴

The ductile iron made was according to ASTM A 536-70, Standard of Class 65-45-12, 65,000 psi minimum tensile strength, 45,000 psi minimum yield strength (with 2% offset) and 12% minimum elongation. The tensile test showed that the ultimate tensile strength and the yield strength were normally well above the set standards mentioned above, but the ductility was very poor and the percent elongations were below the standard value with the exception of the fourth ingot. The results of the first two ingots do not even come close to any of the published standards for North America because of their extremely poor ductility. The loss in ductility could be blamed on the presence of deteriorated and flaky graphite and of carbides in the matrix structure. A minimum of 80% of the matrix structure should be ferritic in order to have 12% elongation.

In common foundry practice, if tests are performed on any specified grade, the foundryman should find considerably higher strength and ductility than the specified minimum. Such a conservative attitude obviously serves the cause of safety, and it also means that most of the castings can be delivered as-cast unless the designer specifies otherwise.

The The physical shape of the castings measurably affects the tensile properties of the metal. The effect of section size on the properties is the result of changes in microscopic structure as the latter is influenced by the solidification time and the cooling rate. Very high cooling rates

do not permit all the insoluble carbon to precipitate in the form of spheroidal graphite; instead, various amounts of iron carbides form. Very slow cooling results in the precipitation of large and irregularly shaped spheroids of graphite.

The results of the tensile tests, shown in figures 20 to 23, can be used to assess the effect of different rates of solidification and cooling on the mechanical properties of the metal. The tensile and yield strength decreased with the increase in the solidification time, with the exception of the first ingot in which the strength increased instead of decreasing. The normalization treatment to the tensile specimens of the first ingot before testing changed the matrix structure from predominantly ferritic to predominantly pearlitic. The heat treatment had no marked effect on the graphite structure. Due to this change in matrix structure the strength must have increased with the relative amount of pearlite formed in each section.

It was rather surprising that the ductility also decreased with an increase in solidification times. No definite reason for such behaviour could be assessed but a few possible explanations for such behaviour could be:

(a) The nodule to flake graphite ratio increased with decreasing solidification times (from section B to F). Therefore, the ductility should also increase with increasing nodule count.

The nodular graphite structure produces a metal which is more ductile and tougher than the flaky structure. The spheroidized microstructure is the tougher of the two because the fracture path must pass

through the tough, deformable ferrite as well as through the graphite nodules. It is also more ductile because there is a greater opportunity for plastic deformation and energy absorption along the path of potential fracture. In contrast, the flaky microstructure is less ductile because there is a more continuous fracture path along graphite flakes.

(b) The very slow cooling of thick metal sections causes the cells to grow to a large size. The formation of very large graphite nodules and a large cell (grain) size can result in increased segregation at the cell boundaries. This reduces the strength and ductility of the iron.

Ingot IV provided the best mechanical properties and microstructure among the four ingots (figure 23). The ultimate strength varied from 76,000 psi to 82,500 psi, whereas the ductility varied from 8.06% to 16.3%. The ductility was below the standard 12% minimum value at section C.

CONCLUSIONS

1. Facilities for rapid chemical analysis of each melt are necessary for the consistent production of good quality ductile iron. The determination of carbon equivalent alone has proved to be insufficient to provide the desired chemical composition.
2. The use of a high percentage of steel scrap in the charge can result in unknown and widely varying compositions of cast iron from melt to melt further necessitating the need for chemical analysis.
3. The cooling rate has a marked effect on the size and the number of graphite nodules. Nodules become relatively finer and more numerous as the cooling rate is increased.
4. Increase in silicon content improved the nodular graphite structure of the ductile iron. Optimum magnesium recovery is very difficult but necessary to obtain the graphite nodular structure.
5. As-cast ductile iron showed a decrease in strength with increase in solidification time (or decrease in cooling rate), whereas the tensile strength of normalized ductile iron increased with the increase in solidification time.
6. The percent elongation of as-cast and normalized ductile iron decreased with increase in solidification time.

7. The chemical composition showed a tremendous effect on the mechanical properties of the ductile iron. Tremendous variations in ductility in particular were observed with the change in chemical composition and graphite morphology.

REFERENCES

1. J. R. Cahoon, University of Manitoba, private communications.
2. H. Morrogh and W. J. Williams, J.I.S.I. 155, 321, (1947).
3. H. Morrogh and W. J. Williams, J.I.S.I. 158, 306, (1948).
4. Stephen I. Karsay, Ductile Iron Production, Quebec Iron and Titanium Corp. (1969).
5. H. E. Henderson, Foundry Trade Journal, Nov. 1966, 673.
6. Charles F. Walton, Grey and Ductile Iron Casting Handbook, Grey and Ductile Iron Founders Society, Cleveland, (1971).
7. Arthur B. Tesmen, Metal Progress, 90, 111, (1966).
8. P. M. Thomas and J. E. Gruzleski, Paper presented at CIM Conference of Metallurgists, Halifax, Nova Scotia, Aug. 27-30, 1972.
9. P. M. Thomas and J. E. Gruzleski, J.I.S.I., June 1973, 426.
10. J. C. Sawyer and J. F. Wallace, Trans. A.F.S., 76, 385, (1968).
11. S. E. Wetterfall, H. Fredriksson and M. Hillert, J.I.S.I. 210, 323, (May 1972).
12. M. Hillert and N. Lange, J.I.S.I. 203, 273, (March 1965).
13. I. C. H. Hughes, Solidification of Metals, I.S.I. London, 184, (1968).
14. B. Lux and W. Kurz, Solidification of Metals, I.S.I. London, 193, (1968).
15. H. Morrogh, Solidification of Metals, I.S.I. London, 238, (1968).
16. G. Jolley, Solidification of Metals, I.S.I. London, 242, (1968).
17. C. R. Loper and R. Heine, Trans ASM, 56, 135, (1963).
18. J. D. Schobel, ASM Seminar on Recent Research on Cast Iron (Ed: H. D. Merchant), 303, New York, Gordon and Breach (1968)
19. Minkoff, Solidification of Metals, I.S.I. London, 251, (1968).
20. W. Oldfield, G. T. Geering and W. A. Tiller, Solidification of Metals, I.S.I. London, 256, (1968).

21. R. W. Ruddle, Journal Institute of Metals, 77, 1, (1950).
22. R. W. Ruddle, The Solidification of Castings, Institute of Metals, (1957).
23. B. E. Jacobs, Jr., Foundry Journal, 122, (Aug. 1966).
24. R. W. Cahn, Physical Metallurgy, John Wiley & Sons Inc., 605, (1965).
25. Stephen I. Karsay, Ductile Iron II, Quebec Iron and Titanium Corporation (1971).